

Impacts of Incoming Shortwave Radiation on Earth's Surface

A Dissertation for

Course Code and Course Title: MSC 617 Discipline Specific Dissertation

Credits: 16

Submitted in partial fulfillment of Master's Degree

M.Sc. In Marine Sciences

By

SAISHA SUBHASH BANDODKAR

Roll Number: 22P0400022

ABC ID: 574831222495

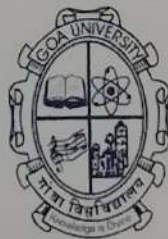
PR Number: 201902254

Under the Supervision of

NIKITA MANGESHKAR

School of Earth, Ocean and Atmospheric Sciences

Marine Sciences



GOA UNIVERSITY

April 2024



Examined by:

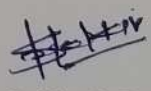
Seal of the School

DECLARATION BY STUDENT

I hereby declare that the data presented in this Dissertation report entitled "Impacts of Incoming Shortwave Radiation on Earth's Surface" is based on the results of investigations carried out by me in the Discipline of Marine Sciences at the School of Earth, Ocean and Atmospheric Sciences, Goa University under the Supervision of Ms. Nikita Mangeshkar and the same has not been submitted elsewhere for the award of a degree or diploma by me. Further, I understand that Goa University or its authorities will not be responsible for the correctness of observations / experimental or other findings given in the dissertation.

I hereby authorize the University authorities to upload this dissertation on the dissertation repository or anywhere else as the UGC regulations demand and make it available to any one as needed.

Date: 26/04/24.
Place: Goa University, Taleigão Plateau, Goa

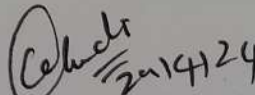

Saisha Subhash Bandodkar
Seat No: 22P0400022

COMPLETION CERTIFICATE

This is to certify that the dissertation report "**Impacts of Incoming Shortwave Radiation on Earth's Surface**" is a bonafide work carried out by **Ms. Saisha Subhash Bandodkar** under my supervision in partial fulfilment of the requirements for the award of the degree of **Master of Science** in the Discipline of Marine Sciences at the School of Earth, Ocean and Atmospheric Sciences, Goa University.

Date: 26/04/2024

Ms. Nikita Mangeshkar
Discipline of Marine Sciences,
School of Earth, Ocean and Atmospheric Sciences


Sr. Prof. Sanjeev C. Ghadi,
Senior Professor and Dean
Marine Sciences
School of Earth, Ocean and Atmospheric Sciences
Date:
Place: Goa University, Taleigão Plateau, Goa



School Stamp

CONTENTS

Chapter	Particulars	Page numbers
	Preface	I
	Acknowledgements	III
	List of Abbreviation	V
	List of Figures	VI
	List of Equations	VII
	Abstract	IX
1	Introduction	1-10
	1.1 Background	
	1.1.1 Absorption	
	1.1.2 Scattering	
	1.1.3 Laws of Radiation	
	1.1.4 Earth's Heat Budget	
	1.2 Aims and Objectives	13
	1.3 Scope	13
2	Literature Review	14-22
3	Data and Methodology	23-24
4	Analysis and Conclusions	25-59
	4.1 Decadal Global Variation	25-30
	4.1.1 Decadal Global Variation of Surface Net Shortwave Solar Radiation from year 2012- 2023	
	4.1.2 Decadal Global Variation of Mean Surface Net Long-wave Radiation Flux from year 2012-2023	
	4.1.3 Decadal Global Variation of Sea Surface Temperature (SST) from year 2012-2023	
	4.2 Monthly Variations in Indian Ocean(1972-	

2023)	
4.2.1 Monthly Variations of Surface Net Solar Radiation in the Indian Ocean (1972-2023)	31-42
4.2.2 Monthly Variation of Mean Surface Net Longwave Radiation Flux from year 1972-2023	
4.2.3 Monthly Variation of Sea Surface Temperature from year 1972-2023	
4.3 Global Time Series Plot: Anomalies in Climate Data (1972-2023)	43-48
4.3.1 Time series plot of Surface Net Shortwave Solar Radiation from year 1972-2023	
4.3.2 Time series plot of Mean Surface Net Longwave Radiation Flux from year 1972-2023	
4.3.3 Time series plot of Sea Surface Temperature (SST) from year 1972-2023	
4.4 Discussion	49-54
4.4.1 Temporal Trends: Shortwave Radiation, Longwave Radiation, and Sea Surface Temperature over Year (1972-2023)	
4.5 Conclusion	55-59
Reference	60-66

PREFACE

Net surface shortwave radiation refers to the balance between incoming shortwave solar radiation (such as sunlight) and outgoing shortwave radiation reflected from the Earth's surface. It's essentially the difference between the amount of solar energy absorbed by the Earth's surface and the amount reflected back into space.

Mean surface net longwave radiation flux, on the other hand, refers to the balance between incoming longwave radiation (mainly from the sun) and outgoing longwave radiation emitted by the Earth's surface. This flux includes both the emission of infrared radiation from the Earth's surface and the absorption and re-emission of longwave radiation by greenhouse gases in the atmosphere. Sea surface temperature (SST) is the temperature of the water at the ocean's surface.

When solar radiation is absorbed by the Earth's surface, it warms the surface and contributes to the heating of the atmosphere and oceans. Longwave radiation helps to regulate the Earth's surface temperature by trapping heat in the atmosphere, known as the greenhouse effect. SST is influenced by both shortwave and longwave radiation. Incoming solar radiation heats the ocean's surface directly, while outgoing longwave radiation from the surface is influenced by the ocean's temperature. Warmer temperatures lead to higher rates of longwave radiation emission.

In the Indian Ocean, shortwave radiation varies seasonally with solar insolation and is affected by cloud cover and aerosols. Longwave radiation is influenced by sea surface temperature, atmospheric conditions, and greenhouse gas concentrations. Sea surface temperature exhibits spatial and temporal variability driven by equatorial warming,

monsoon winds, and upwelling zones, impacting regional climate dynamics and marine ecosystems.

Understanding these fluxes helps scientists model and predict climate changes and variations in the Earth's temperature over time. For instance, if there's an imbalance between incoming and outgoing radiation, it can lead to changes in the Earth's temperature, affecting weather patterns, ocean currents, and ultimately, the climate. This motivated me on the topic “Impacts of Incoming Shortwave Radiation on Earth’s Surface”

ACKNOWLEDGEMENTS

I would like to express my heartfelt gratitude to the God for granting me the strength throughout the journey of completing this dissertation. I extend my deepest appreciation to my family for their support.

A special word of thanks goes to my guide Ms. Nikita Mangeshkar, Assistant Professor, at the School of Earth, Ocean and Atmospheric Sciences, Goa University, for her invaluable support and guidance throughout the dissertation process. Her expertise, patience, and encouragement have been instrumental in shaping this work and navigating through its complexities.

I would like to thank Sr. Prof. Sanjeev C. Ghadi, Dean of School of Earth, Ocean and Atmospheric Sciences, Goa University and Sr. Prof. C. U. Rivonker, Former Dean of School of Earth, Ocean and Atmospheric Sciences, for providing with the necessary facilities that aided in the completion of my dissertation work.

Additionally, I would like to thank the data providers –The data is of Surface Net Shortwave Solar Radiation, Mean Surface Net Longwave Radiation Flux and Sea Surface Temperature from ERA5. The data was downloaded from the webpage:

<https://cds.climate.copernicus.eu/cdsapp#!/dataset/reanalysis-era5-single-levels-monthly-means?tab=form>

I would also like to extend my heartfelt appreciation to my dear friend Ms. Ashis Karthika for her assistance and support. Her willingness to lend a helping hand, offer

insightful advice, is deeply appreciated. To everyone who has played a part, no matter how big or small, in this journey, I offer my sincere gratitude.

LIST OF ABBREVIATIONS

Entity	Abbreviation
Ultraviolet	UV
Nanometer	nm
Near-infrared	NIR
Millimeter	mm
Ozone	O ₃
Oxygen	O ₂
Kelvin	K
Micrometer	μm
Sea Surface Temperature	SST
General Circulation Model	GCM
Moderate Resolution Imaging Spectroradiometer	MODIS
Snow Water Equivalent	SWE
Earth Radiation Budget Experiment	ERBE
Earth Radiation Budget Satellite	ERBS
Passive Microwave	PMW
Marine Heat Waves	MHWs
Ocean Thermal Energy Conversion	OTEC
Joules per square meter	J/m ²
Watts per square meter	W/m ²
Degree Celsius	°C
Carbon dioxide	CO ₂
Methane	CH ₄
Nitrous oxide	N ₂ O

LIST OF FIGURES

Figure number	Description	Page number
4.1.1	Decadal Global Variation of Surface Net Shortwave Solar Radiation from year 2012-2023.	25
4.1.2	Decadal Global Variation of Mean Surface Net Long-wave Radiation Flux from year 2012-2023.	27
4.1.3	Decadal Global Variation of Sea Surface Temperature (SST) from year 2012-2023.	29
4.2.1	Monthly Variation of Surface Net Solar Radiation in the Indian Ocean from year 1972-2023.	31
4.2.2	Monthly Variation of Mean Surface Net Long-wave Radiation Flux in the Indian Ocean from year 1972-2023.	35
4.2.3	Monthly Variation of Sea Surface Temperature (SST) in the Indian Ocean from year 1972-2023.	39
4.3.1	Global Time series plot of Surface Net Shortwave Solar Radiation from year 1972-2023	43
4.3.2	Global Time series plot of Mean Surface Net Longwave Radiation Flux from year 1972-2023	45
4.3.3	Global Time series plot of Sea Surface Temperature from year 1972-2023	47
4.4.1	Temporal Trends: Shortwave Radiation, Longwave Radiation, and Sea Surface Temperature Over Year (1972-2023)	49

LIST OF EQUATIONS

1. KIRCHHOFF'S LAW: The equation representing Kirchhoff's law for thermal radiation is:

$$\varepsilon (\lambda, T) = \alpha (\lambda, T),$$

Where, ε is the emissivity of the material (greenhouse gas) at wavelength λ and temperature T;

α is the absorptivity of the material (greenhouse gas) at wavelength λ and temperature T.

2. ENERGY CONSERVATION LAW: Mathematically, this can be represented as:

$$S_{in} = S_{out} + \Delta Q$$

Where, S_{in} represents the incoming solar radiation;

S_{out} represents the outgoing thermal radiation emitted by Earth;

ΔQ represents other energy fluxes, such as energy absorbed or emitted through processes like evaporation, condensation, and human activities.

3. STEFAN BOLTZMANN LAW: Mathematically, it's expressed as:

$$E = \sigma T^4$$

Where, E is the total energy emitted per unit surface area;

σ is the Stefan-Boltzmann constant approximately ($5.67 \times 10^{-8} \text{ W m}^{-2}\text{K}^{-4}$);

T is the absolute temperature of the object in Kelvin.

4. WEIN'S DISPLACEMENT LAW: Wien's displacement law is given by the equation:

$$\lambda_{max} = b/T$$

Where, λ_{\max} is the wavelength at which the spectral radiance of the body is at maximum;

b is Wien's displacement constant, approximately equal to 2.898×10^{-3} m K;

T is the absolute temperature of the object in Kelvin.

ABSTRACT

This study utilizes ERA5 monthly averaged data to analyze the decadal global variation of surface net shortwave solar radiation, mean surface net longwave radiation flux, and sea surface temperature from 2012 to 2023, employing Python programming to generate contour plots. Subsequently, the same dataset is examined over the Indian Ocean from 1972 to 2023, highlighting monthly fluctuations in shortwave radiation, longwave radiation, and sea surface temperature. Global time series plots spanning from 1972 to 2023 are constructed to elucidate trends in these variables, illustrating their collective impact on Earth's heat budget, and impacts of shortwave radiation on earth's surface.

INTRODUCTION

1.1 Background

The Earth's surface is continuously exposed to solar radiation, which serves as the primary energy source for supporting life and driving various planetary mechanisms. This solar radiation, commonly known as insolation, is crucial in molding Earth's climate, guiding weather phenomena, and facilitating vital ecological functions. As solar radiation reaches Earth, it imparts energy through electromagnetic waves, which are absorbed by the atmosphere, land, and oceans. This absorption results in the transformation of solar energy into heat, impacting temperature fluctuations and atmospheric circulation worldwide (*Klassen et al., 2005*).

Various surfaces interact with solar radiation differently, as dark surfaces like forests and oceans tend to absorb more radiation compared to lighter surfaces such as ice and sand, which reflect a greater portion of incoming energy. The significance of insolation goes beyond just regulating temperature; it is essential for sustaining life on Earth. Photosynthesis, a fundamental process in the food chain, relies on solar radiation to convert carbon dioxide and water into glucose and oxygen, thus supporting ecosystems and enriching the atmosphere with oxygen. Solar radiation drives the water cycle by initiating evaporation from water bodies, leading to cloud formation and precipitation, crucial for maintaining freshwater resources and supporting terrestrial life (*Ni et al., 1997*).

Shortwave radiation, which includes ultraviolet (UV) has wavelengths ranging from 10 nanometers (nm) to 400 nanometers (nm). UV radiation is divided into three categories

based on wavelength: UV-A (400 to 315 nm), UV-B (315 to 280 nm), and UV-C (280 to 10 nm) and the visible spectrum have wavelengths ranging from about 400 nanometres (nm) to 700 nanometres (nm), whereas near-infrared (NIR) radiation has wavelengths ranging from about 700 nanometres (nm) to 1 millimeter (mm). It's just beyond the range of what our eyes can see as visible light, which is essential for Earth's energy balance. UV radiation is vital for vitamin D synthesis and photosynthesis but can pose health risks with excessive exposure. Visible light enables illumination, colour perception, and plant photosynthesis. NIR radiation, although invisible, plays a critical role in heating the Earth's surface and remote sensing applications. Understanding shortwave radiation is crucial for comprehending Earth's energy budget, informing climate models, and predicting future climate conditions. Instruments like pyrometers and radiometers allow accurate measurement of solar radiation, vital for monitoring environmental changes and evaluating their impacts (*Swift et al., 2011*).

it into heat, contributing to warming. Conversely, surfaces with high albedo, like ice and snow, reflect more radiation into space, mitigating heat absorption and potentially leading to cooling effects.

1.1.2 Scattering:

Shortwave radiation experiences scattering as it interacts with particles and molecules in the atmosphere. Rayleigh scattering, occurs when radiation interacts with particles much smaller than the wavelength of light (such as nitrogen and oxygen molecules), and gives the sky its blue colour. It contributes to the overall brightness of the atmosphere. Mie scattering, on the other hand, occurs when radiation interacts with larger particles like aerosols and dust particles, redirecting radiation in various directions and influencing the amount reaching the Earth's surface.

1.1.3 Laws of Radiation:

Kirchhoff's Law: There are radiation laws which help us to understand Earth's Heat Budget. One of them is the Kirchhoff's Law that helps us understand the absorption and emissions of the greenhouse gases in the atmosphere.

The equation representing Kirchhoff's law for thermal radiation is given as:

$$\varepsilon (\lambda, T) = \alpha (\lambda, T)$$

Where, ε is the emissivity of the material (greenhouse gas) at wavelength λ and temperature T; α is the absorptivity of the material (greenhouse gas) at wavelength λ and temperature T.

This law implies that gases that effectively absorb radiation (high absorptivity) also emit radiation efficiently (high emissivity) at the same wavelengths and temperatures

Greenhouse gases like water vapour and carbon dioxide have high absorptivity for longwave infrared radiation emitted by Earth's surface, trapping heat and leading to the warming of the lower atmosphere causing global temperatures to increase. This absorbed energy is then re-radiated in all directions, including back towards the Earth's surface. This phenomenon, often referred to as the greenhouse effect, helps maintain the Earth's surface temperature at a level suitable for supporting life. Anthropogenic activities, particularly the burning of fossil fuels and deforestation, have led to an increase in the concentration of greenhouse gases in the atmosphere, especially carbon dioxide and methane. This phenomenon is commonly known as global warming and is a major driver of global climate change.

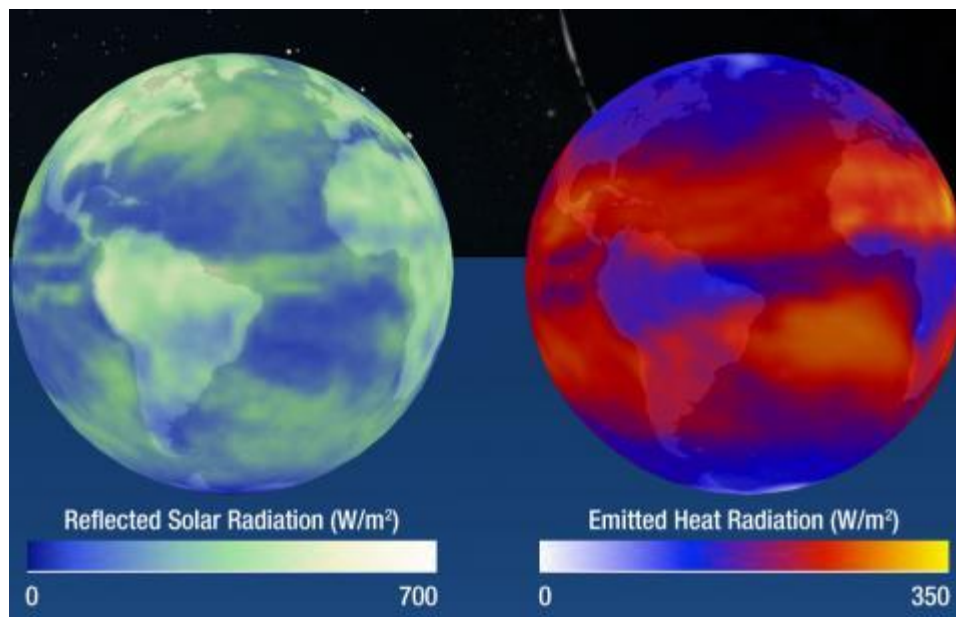


Figure 1.2: The spatial variability in average segregated by atmosphere and earth surface reflected and emitted radiation from earth's surface (NASA 2010)

(<https://mydasdata.larc.nasa.gov/basic-page/earths-energy-budget>)

In the figure 1.2, on the left, the sphere is labeled "Reflected Solar Radiation (W/m²)" with a scale at the bottom ranging from 0 to 700 W/m². The colours on this sphere range from blue to green, suggesting varying levels of solar radiation being reflected by different parts of the Earth's surface or atmosphere.

On the right, the sphere is labeled "Emitted Heat Radiation (W/m²)" with a scale at the bottom ranging from 0 to 350 W/m². This sphere uses a color palette ranging from blue to red, indicating different levels of heat radiation emitted from the Earth's surface or atmosphere.

They compare the distribution of reflected solar radiation and emitted heat radiation across the Earth's surface. The colour gradients on each sphere are used to visually

represent the intensity of radiation in different regions, with cooler colours typically representing lower values and warmer colours representing higher values.

Energy Conservation Law: Based on the conservation of energy principle we can understand Earth's heat budget. Earth's heat budget signifies the equilibrium between incoming solar radiation absorbed by the planet and outgoing thermal radiation emitted back into space. According to this principle, the incoming energy must equal the outgoing energy for the Earth's temperature to maintain relative stability over time.

This principle is often expressed as:

$$\text{Incoming solar radiation} = \text{outgoing thermal radiation} + \text{other energy fluxes}$$

Mathematically, this can be represented as:

$$S_{\text{in}} = S_{\text{out}} + \Delta Q$$

Where, S_{in} represents the incoming solar radiation; S_{out} represents the outgoing thermal radiation emitted by Earth and ΔQ represents other energy fluxes, such as energy absorbed or emitted through processes like evaporation, condensation, and human activities.

Stefan-Boltzmann Law: The heat budget is described in terms of energy fluxes, representing rates of energy transfer, at different stages of the Earth-atmosphere system. Stefan-Boltzmann Law is highly relevant to Earth's heat budget. The law states that the total energy emitted per unit surface area of a black body (or an idealized perfect emitter of radiation) is directly proportional to the fourth power of its absolute temperature.

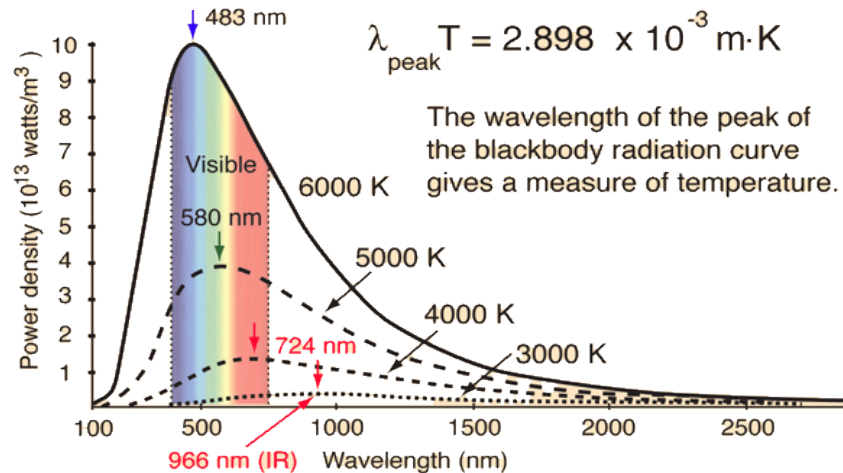
Mathematically, it's expressed as:

$$E = \sigma T^4$$

Where, E is the total energy emitted per unit surface area; σ is the Stefan-Boltzmann constant approximately ($5.67 \times 10^{-8} \text{ W m}^{-2}\text{K}^{-4}$); and T is the absolute temperature of the object in Kelvin.

This law helps us understand how much thermal radiation Earth emits into space based on its temperature. Earth's surface temperature is around 288 Kelvin, and using the Stefan-Boltzmann Law, we can calculate the total energy emitted per unit surface area. This emitted thermal radiation is a crucial component of Earth's heat budget. It represents the energy that the Earth loses to space and plays a significant role in maintaining the planet's overall temperature balance. Together with incoming solar radiation, which heats the Earth, the outgoing thermal radiation governs the Earth's energy balance and influences its climate.

Wien's displacement law: relates the peak wavelength of the radiation emitted by an object to its temperature. Although originally formulated for blackbody radiation, it can also be applied to solar radiation.



<http://hyperphysics.phy-astr.gsu.edu/hbase/wien.html>

Wien's displacement law is given by the equation:

$$\lambda_{\text{max}} = b/T$$

Where, λ_{max} is the wavelength at which the spectral radiance of the body is maximum; b is Wien's displacement constant, approximately equal to $2.898 \times 10^{-3} \text{ m K}$; and T is the absolute temperature of the object in Kelvin.

For solar radiation, the temperature T refers to the effective temperature of the Sun's photosphere, which is around 5778 K. By substituting this value into the equation, you can find the peak wavelength of solar radiation.

1.1.4 Earth's Heat Budget:

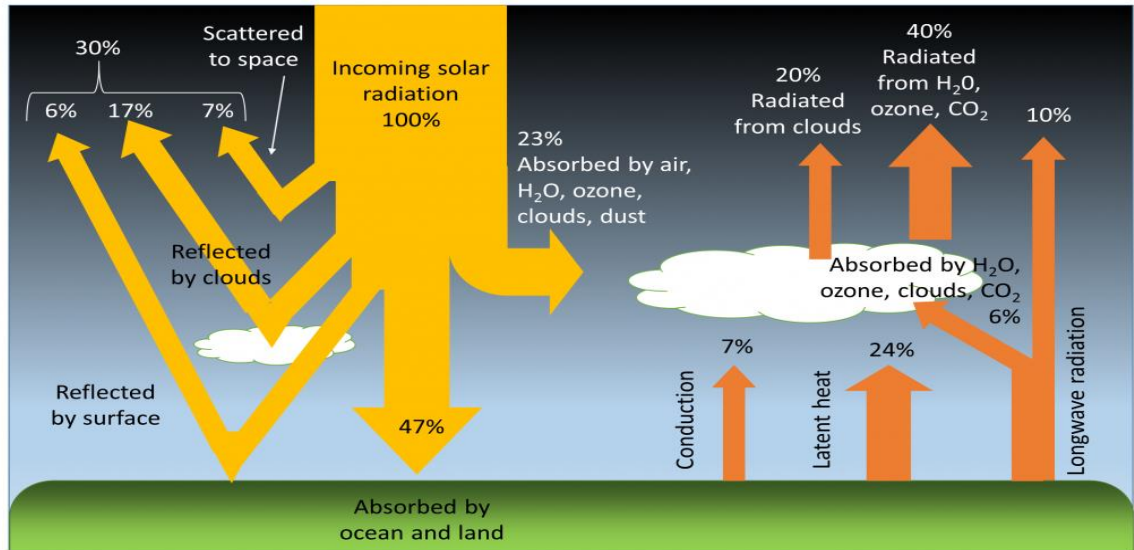


Figure 1.3: Earth's Heat Budget

(<https://rwu.pressbooks.pub/webboceanography/chapter/8-1-earths-heat-budget/>)

The incoming solar radiation is distributed in the following manner:

- Solar radiation encompasses ultraviolet (about 5%), visible (around 40%), and infrared (approximately 55%) segments of the electromagnetic spectrum.
- The ozone layer in the upper atmosphere absorbs radiation with wavelengths shorter than 0.29 μm , shielding life on Earth from harmful cosmic and UV rays.
- When considering the total shortwave radiation received at the top of the atmosphere as 100%, approximately 35% is reflected into space under clear sky conditions.
- Factors contributing to shortwave scattering into space include cloud droplets (27%), atmospheric gas molecules (6%), and snow or ice-covered areas of the Earth (2%).

- The remaining 65% of shortwave radiation is absorbed by the Earth's atmosphere, with 14% by the atmosphere itself and 51% by the Earth's surface.
- With 35% of insolation reflected as albedo, the balance of 65% of shortwave radiation contributes to longwave radiation.
- Regarding longwave radiation, the Earth's surface emits 51% of terrestrial radiation, with 17% directly radiated to space and the remaining 34% absorbed by the atmosphere.
- Of the 34% absorbed by the atmosphere, 6% is absorbed directly, 9% through convection and turbulence, and 19% through the latent heat of condensation.
- Daytime insolation is the primary source of the remaining 14% of longwave radiation.
- Ultimately, 48% of terrestrial longwave radiation is absorbed by the atmosphere, which, combined with the 14% from insolation, constitutes the total radiation returned from the Earth and atmosphere, balancing the net 65% of shortwave radiation received from the sun.

The Earth's heat budget is dynamic and continually changing due to natural variability and anthropogenic activities like deforestation, urbanization, and the combustion of fossil fuels. Alterations in the Earth's heat budget can lead to shifts in global climate patterns, including temperature fluctuations, changes in precipitation patterns, and variations in the frequency and intensity of extreme weather events. The interaction of shortwave radiation (solar radiation) over terrestrial (land) and oceanic (ocean) regions differs due to variations in surface properties such as albedo, heat capacity, and moisture content.

The relationship between shortwave radiation and sea surface temperature (SST) is complex and multifaceted, in which shortwave radiation influences SST in the following ways:

1. Shortwave radiation from the Sun penetrates the ocean surface and heats the water. The amount of shortwave radiation absorbed by the ocean depends on factors such as solar angle, cloud cover, and atmospheric conditions. Higher levels of shortwave radiation can lead to increased SST by providing more energy for heating the water.
2. Shortwave radiation plays a role in driving ocean circulation patterns. Warm surface water heated by shortwave radiation tends to move away from the equator toward the poles, while cooler waters from higher latitudes move toward the equator. This circulation redistributes heat around the globe and influences SST patterns.
3. Changes in SST can, in turn, influence shortwave radiation. Warmer sea surface temperatures can lead to increased evaporation, cloud formation, and changes in atmospheric circulation patterns. These changes can affect the amount and distribution of shortwave radiation reaching the ocean surface.
4. SST influences marine ecosystems, including the distribution and behaviour of marine organisms. Changes in SST due to variations in shortwave radiation can impact the productivity of phytoplankton, the distribution of fish species, and the occurrence of marine heat-waves, among other factors.

1.2 AIMS AND OBJECTIVES

- To understand the shortwave radiation, longwave radiation and sea surface temperature over global region and Indian Ocean.
- To study variability of shortwave radiation, longwave radiation and sea surface temperature for last 50 years and its impact.

1.3 SCOPE

The study enables the understanding of the interplay between shortwave radiation (incoming solar radiation) and longwave radiation (outgoing thermal radiation) with sea surface temperature (SST) changes.

It can help in exploring the implications of SST variability and changes in radiation balance on marine ecosystems in the Indian Ocean and globally as well as in investigating the feedback mechanisms between radiation balance, SST, and the atmosphere-ocean system. For example, warmer SSTs can lead to increased water vapour in the atmosphere, which in turn affects cloud cover and radiation balance.

The study will help evaluate the socio-economic impacts of the changes in shortwave radiation, longwave radiation, and SST, particularly for coastal communities, fisheries, agriculture, and water resources management in the Indian Ocean region and beyond; and will help in developing predictive models to project future changes in shortwave radiation, longwave radiation, and SST under different emissions scenarios. This could involve using climate models and statistical techniques to simulate future climate conditions and assess associated risks.

CHAPTER 2 : LITERATURE REVIEW

Shortwave radiation from the sun, which includes factors like the angle of sunlight, cloud cover, and aerosols in the atmosphere, is the primary energy source for Earth's climate system. It plays a crucial role in determining temperature changes and trends by influencing how much heat is absorbed or reflected by the planet (*Budyko et al., 1969*). Incoming longwave radiation measures the amount of thermal radiation emitted by the Earth's surface and then reflected into the atmosphere. This radiation interacts with atmospheric components like clouds, water vapour, and greenhouse gases. These factors determine how much of this radiation is absorbed and re-emitted within the atmosphere. It's influenced by atmospheric conditions like cloud cover, water vapour levels, and the concentration of greenhouse gases. The radiation contributes to both short-term weather changes and long-term climate patterns (*Webster et al., 1981*). The albedo, which refers to the reflectivity of Earth's surface, is vital in deciding how much of the incoming shortwave radiation from the sun is bounced back into space. This is particularly important in regions where there are seasonal changes between snow-covered and snow-free conditions, as it greatly affects temperature patterns. Changes in albedo caused by global warming can lead to notable local effects, like polar amplification, where temperature changes are more pronounced at the poles. These alterations in albedo can also have far-reaching consequences across larger geographic areas (*Ellis et al., 1999*). Soil moisture is pivotal in deciding how net radiation is distributed between sensible heat flux (directly heating the air) and latent heat flux (evaporation). This distribution significantly impacts near-surface air temperature, especially in various regions worldwide, particularly during summer (*Miralles et al., 2012*).

In the study “Incoming Shortwave Fluxes at the Surface, a Comparison of GCM Results with Observations”, Garratt et al., 1994, studied comparison of surface net radiation from General circulation models (GCM) and observations carried from 22 worldwide inland stations. The focus was on understanding the discrepancies between the modeled and observed values of net radiation and incoming shortwave fluxes at the Earth's surface. The findings suggested that the overestimation in models of net radiation on an annual basis is mainly attributed to excess incoming shortwave fluxes. By comparing the results from four GCMs with long-term observations, the study quantified these differences. It indicated that the overestimation of net radiation by the models is around 20% annually, while the overestimation for shortwave fluxes alone was approximately 6% for the same set of locations. The study suggested that these differences between model predictions and observations are significant, especially when considering the larger dataset of 93 stations, where the discrepancy in shortwave fluxes accounts for a 9% overestimation. The research underscored the importance of accurately representing incoming shortwave fluxes in GCMs to improve the reliability of their predictions regarding surface net radiation.

The study of “Slope effects on shortwave radiation components and net radiation” done by Walter et al.,1992, highlighted significant discrepancies between General Circulation Models (GCMs) and observed data regarding surface net radiation and incoming shortwave fluxes. These differences are primarily attributed to an overestimation in models, particularly regarding net radiation, with excess incoming shortwave fluxes being a major contributing factor. The study underscored the importance of accurately

representing incoming shortwave fluxes in GCMs to enhance the reliability of their predictions concerning surface net radiation.

The study on “Spatial variability of shortwave radiative fluxes in the context of snowmelt”, conducted by Hinkelman et al., 2014, utilized observations from the Moderate Resolution Imaging Spectroradiometer (MODIS) to analyze the spatial variability of shortwave radiative fluxes in complex terrain, particularly focusing on the impact of slopes on the amount of radiation received. The methodology developed in this study has been applied to multiple water years (January to July 2003, 2004, 2005, and 2009) over the western part of the United States. The main objective of the study was to derive metrics on spatial and temporal variability in shortwave fluxes using high spatial resolution (5-km) MODIS data. The ultimate goal was to utilize these findings to improve estimates of Snow Water Equivalent (SWE). By understanding how shortwave radiation varies across complex terrain, researchers had aim to enhance the accuracy of SWE estimates, which are crucial for water resource management, particularly in regions where snowmelt significantly contributes to water supply.

In snow-covered mountain ranges, net radiation typically accounts for around 80% of the energy balance. This net radiation is mainly composed of shortwave radiation from the sun (*Pinker et al., 2014*). Shortwave radiative fluxes play a crucial role in shaping different elements of Earth's climate system, influencing atmospheric and oceanic circulations, as well as surface climate conditions (*Whitlock et al., 1995*). Shortwave radiation finds extensive application in diverse fields like wireless communications, radar observations, industrial processes, and medical treatments. However, it also

presents risks to humans because of its potential to harm biological systems (*Yuet et al., 2017*).

The article “Biological effects and mechanisms of shortwave radiation” which was by Peng et al., 2017, focused on examining the biological effects of shortwave electromagnetic radiation, synthesizing evidence from various research types including in vitro, in vivo, and epidemiological studies. It discussed the mechanisms of interaction with biological systems, and potential health risks, and suggested protective measures. The goal was to provide a comprehensive understanding of shortwave radiation's impact and inform both researchers and policymakers about associated health risks and protective strategies.

Satellite missions and re-analyses provided alternative sources of shortwave radiation data, but their utilization requires validation due to inherent uncertainties (*Sinitsyn et al., 2017*). The study “Shortwave flux at the surface of the Atlantic Ocean: in-situ measurements, satellite data and parameterization” by Alexey et al., 2017, compared three sources of shortwave flux estimates i.e. the in-situ measurements, satellite data, and parameterizations of shortwave fluxes. This comprehensive comparison provided insights into the accuracy and reliability of different methods for estimating shortwave radiation over the surface of the Atlantic Ocean. The comparison revealed that satellite data have a positive bias and RMS compared to in-situ measurements, indicating some discrepancies between the two sources. Additionally, the study evaluated different parameterization schemes for estimating shortwave radiation from cloud observations and identified the IORAS/SAIL scheme as the least biased among the tested algorithms. This evaluation highlighted the importance of assessing the performance of satellite data

and parameterization methods for improving the accuracy of shortwave radiation estimates in oceanic regions.

A sophisticated radiation parameterization scheme has been devised specifically for subgrid topography in mountainous regions. This scheme takes into consideration several factors including shading, restricted sky view, terrain reflections, slope, sun elevation angle, and albedo. By incorporating these factors, the scheme enhances the accuracy of representing the shortwave radiation balance at the surface, providing a more comprehensive understanding of radiation dynamics in mountainous terrain (*Helbig et al., 2012*).

The study “Shortwave Radiation” by Klassen et al., 2005, focused on the importance of accurate shortwave radiation data for evapo-transpiration models used in agricultural applications. It highlighted the suitability of low-cost silicon cell pyranometers for widespread use in unobstructed daylight conditions, while more expensive thermopile pyranometers are necessary for specific light conditions. The study emphasized routine maintenance practices such as cleaning, levelling, and annual calibration checks to ensure the integrity of long-term data.

Comparisons between tungsten lamp and solar calibration measurements provided valuable insights into the accuracy and reliability of the calibration process for the Earth Radiation Budget Experiment (ERBE) active cavity radiometers located on NASA's Earth Radiation Budget Satellite (ERBS) and the NOAA-9 and NOAA-10 spacecraft platforms (*Thomas et al., 1992*). According to Sedlar et al., 2017, while previous studies have primarily focused on the role of enhanced poleward atmospheric transport of

moisture and heat during spring as a key preconditioning mechanism for Arctic sea ice melt, recent observations from state-of-the-art satellite sensors suggested that shortwave radiation may also play a significant role in springtime Arctic atmospheric preconditioning, challenging previous conclusions derived from atmospheric reanalysis data.

At high latitudes, longwave radiation can provide similar, or higher, amounts of energy to snow than shortwave radiation due to the low solar elevation (cosine effect and increased scattering due to long atmospheric path lengths). This effect is magnified in mountains due to shading and longwave emissions from the complex topography (*Sicart et al., 2006*). Accurate knowledge of global sea surface temperature (SST) distribution and temporal variation is crucial for various applications, including forecasting and prediction systems, maritime safety, military operations, ecosystem assessment, supporting fisheries and tourism, transport and energy, human health, food security, and environmental policy (*Robinson et al., 2012*).

Understanding oceanic and atmospheric processes relies on knowledge of the temperature at which these processes occur. This includes processes such as radiative emission, gas solubility (including CO₂), evaporation, and sensible heat flux, all of which are influenced by the temperature at the ocean surface (*Lindzen et al., 1987*). Sea surface temperature (SST) are obtained through different methods, including in situ contact thermometers and remote sensing using infrared (IR) and passive microwave (PMW) radiometers on satellites. These methods offer complementary characteristics, with IR-derived SST being cooler than the water beneath by approximately 0.17 K on average, while PMW-derived SSTs have the advantage of being less influenced by

cloud cover due to the propagation of microwave radiation (*Donlon et al., 2002; Minnett et al., 2011*). Merging data from both IR and PMW sensors, along with in situ measurements, is a widely accepted approach to derive global SST fields (*Chin et al., 2017*).

Studies have detected positive trends in both SST and air temperature in regions such as the Adriatic Sea, with implications for marine fauna and the population and development of coastal areas. Additionally, phenomena like El Niño events can be studied through SST analysis. Future climate scenarios, including SST evolution, are of particular interest, with projections indicating significant increases in SST in certain regions by 2100. Furthermore, marine heat waves (MHWs) have emerged as a poorly studied phenomenon gaining attention in ocean science literature. The frequency and intensity of MHWs have increased in recent decades, impacting marine biodiversity and becoming a major focus of study (*Pastor et al., 2021*). Sea surface temperature (SST) serves as a fundamental climatic index, allowing for the assessment of the ocean's current state and the evaluation of climate change impacts on a regional scale. SST moderates the heat interaction between the ocean and the atmosphere, playing a crucial role in reflecting sea surface salinity and modifications in ocean thermohaline motion (*Pisano et al., 2020*).

Distinction between the methods used to measure sea surface temperature (SST). Traditional methods involve mercury-in-glass thermometers in buckets or thermistors on buoys, which measure the "bulk" SST at depths of tens of centimeters to a few meters. More recently, remotely sensed measurements from satellite infrared radiometers provide SST measurements close to the sea surface, known as the "skin

temperature." This skin temperature is significant as it reflects the temperature of the ocean in direct contact with the atmosphere, playing a crucial role in controlling heat and gas transfers between the ocean and the atmosphere. This highlights the importance of considering both bulk and skin SST measurements in understanding ocean-atmosphere interactions (*Minnett et al., 2015*).

The appropriate measure of sea surface temperature (SST) for determining longwave radiation is the skin temperature. This skin temperature refers to the literal surface of the sea, which is less than one millimeter thick. Longwave radiation emitted from the sea surface depends mainly on this skin temperature because water is nearly opaque to longwave radiation, and incoming longwave radiation from the atmosphere is absorbed in the top millimeters of the water column. As a result, the outward longwave radiation is primarily influenced by the temperature of this thin surface layer (*Swift et al., 2011*).

The temperature difference between the warm surface water and cold deep ocean water in certain regions allows for the potential utilization of ocean thermal energy conversion (OTEC) plants. These plants convert thermal energy from the ocean into electricity by harnessing the temperature gradient. OTEC represents a promising renewable energy source, tapping into the vast thermal energy reservoir of the ocean (*Mohammed et al., 2011*).

Flux towers play a crucial role in studying the surface heat budget. These towers are equipped with rapid response instruments that measure various atmospheric parameters such as air temperature, humidity, vertical air speed, and components of long and shortwave radiation. Using the eddy correlation method, flux towers can determine

sensible and latent heat fluxes, providing valuable insights into the heat exchange processes occurring at the Earth's surface. Additionally, a few temperature sensors in the ground can help estimate heat storage, contributing to a comprehensive understanding of the surface energy balance (*Smith et al., 2010*).

The ocean energy budget, governed by the first law of thermodynamics, involves the rate of change of the internal energy of the ocean system being equal to the net heat flux through its boundaries. This internal energy, represented by the temperature structure of the ocean, is crucial in understanding thermal energy gains and losses within the ocean. It's emphasized that the total thermal energy entering the ocean must balance with the total thermal energy lost to prevent significant temperature changes over time (*Fiazal et al., 2011*). Various forms of thermal energy contribute to the ocean heat budget, such as conduction through the ocean bottom and heat generated from ocean currents; these are often neglected due to their small magnitude compared to solar energy input (*Ahmed et al., 2011*).

CHAPTER 3 : DATA AND METHODOLOGY

ERA5 (ECMWF Reanalysis 5) is a state-of-the-art atmospheric reanalysis dataset produced by the European Centre for Medium-Range Weather Forecasts (ECMWF). It provides comprehensive information about various atmospheric variables on a global scale, including temperature, humidity, wind, pressure, and more. Single level refers to data that is interpolated or averaged to a specific altitude or pressure level in the atmosphere, such as surface level or a fixed altitude above the surface. Daily averaged means that the data is averaged over a 24-hour period, typically from midnight to midnight UTC (Coordinated Universal Time), providing daily values for each variable.

ERA5 single level daily averaged reanalysis data would include atmospheric variables averaged over a single level (e.g., surface level) and averaged over daily intervals, providing a comprehensive picture of atmospheric conditions over time. This type of data is valuable for various applications, including climate monitoring, research, and weather forecasting.

Data was downloaded from ERA5 single level daily averaged data from year 1972 to 2023. Website: <https://cds.climate.copernicus.eu/cdsapp#!/dataset/reanalysis-era5-single-levels-monthly-means?tab=form>

Initially, data for global region of Surface net shortwave solar radiation spanning from 1972 to 2023 was downloaded in an NC file format. After downloading, the files were renamed for organizational convenience. Subsequently, an analysis code was developed to process this data. Using Python, contour plots were generated for each decade (i.e., every 10years) to visualize the trends over time for surface net shortwave solar

radiation. Following a similar procedure, contour plots were also created for sea surface temperature and mean surface net long-wave radiation flux.

After the contour plots, Time series plot for surface net shortwave solar radiation, sea surface temperature and mean surface net long-wave radiation flux over global region was plotted from year 1972-2023. The methodology for generating time series plots of surface net shortwave solar radiation, sea surface temperature, and mean surface net long-wave radiation flux over a global region involved two main steps using Python. Initially, average values were computed for each variable using dedicated code. Subsequently, these averaged values spanning from the year 1972 to 2023 were utilized as inputs in separate code to construct the time series plots.

The monthly variation in the Indian Ocean spanning from 1972 to 2023 was depicted through a plotted analysis. Initially, the data was categorized based on monthly averages. For instance, data solely from January across the years 1972 to 2023 was isolated and averaged, repeating this process for all twelve months. Subsequently, contours were plotted for each month to assess the fluctuations in surface net shortwave solar radiation, mean surface net longwave radiation flux, and sea surface temperature.

CHAPTER 4 : ANALYSIS AND CONCLUSION

4.1 Decadal Global Variation

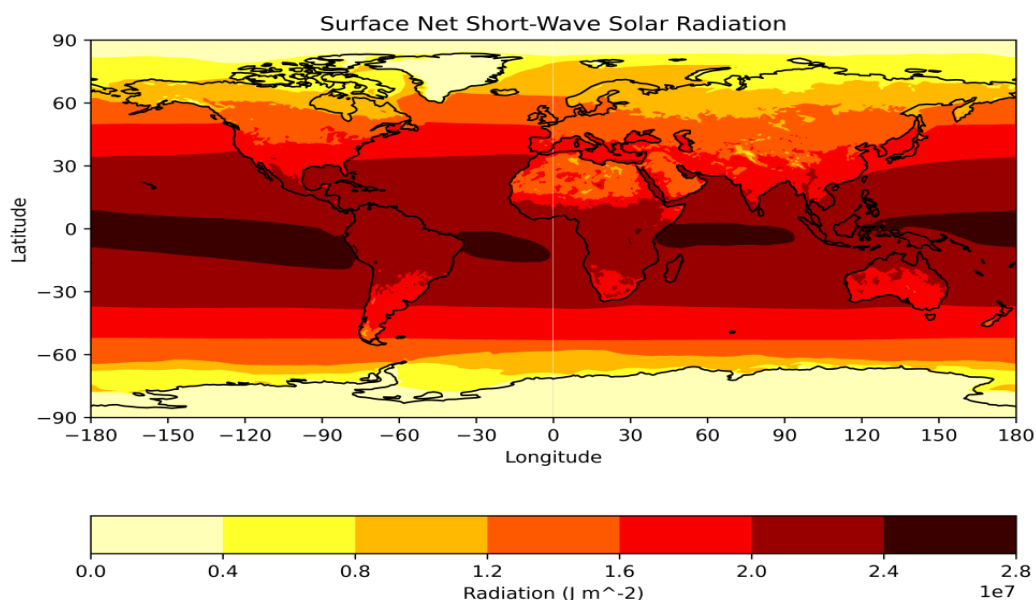


Figure 4.1.1 Decadal Global Variation of Surface Net Shortwave Solar Radiation from year 2012-2023

In figure 4.1.1 contour plot shows the distribution of solar radiation received at the Earth's surface after accounting for the reflection and absorption by the atmosphere.

The latitude and longitude are marked with negative and positive signs to indicate their direction relative to the Equator and the Prime Meridian, respectively. Latitude values are negative in the Southern Hemisphere and positive in the Northern Hemisphere.

Longitude values are negative to the west of the Prime Meridian (which passes through Greenwich, London) and positive to the east.

The scale for the solar radiation plot is shown at the bottom, with a range from 0 to 2.8×10^7 Joules per square meter (J m^2). The colours represent different levels of radiation, with yellow shades indicating lower values and red shades indicating higher values. The highest values of solar radiation are shown in dark red and are most prominent around the equatorial regions which range from 2.4×10^7 to $2.8 \times 10^7 \text{ J m}^2$; this is expected due to the more direct angle of sunlight in these areas. In the tropical region the shortwave radiation is comparatively less than the equator values ranging from 2.0×10^7 to $2.4 \times 10^7 \text{ J m}^2$ whereas in the subtropical region the solar radiation is moderate values ranging from $0.8 \times 10^7 \text{ J m}^2$ to $2.0 \times 10^7 \text{ J m}^2$. And the lowest radiation are shown in yellow and are found towards the poles ranges from $0.8 \times 10^7 \text{ J m}^2$ to 0 m^2 , where the angle of sunlight is more oblique and thus less intense.

The highest value on the scale is $2.8 \times 10^7 \text{ J m}^2$, and the lowest value is 0 J m^2 . The distribution of solar radiation is not uniform across the globe, with the highest values typically found in tropical regions where the sun's rays are most direct, and lower values at higher latitudes where the sun's rays are more spread out due to the curvature of the Earth.

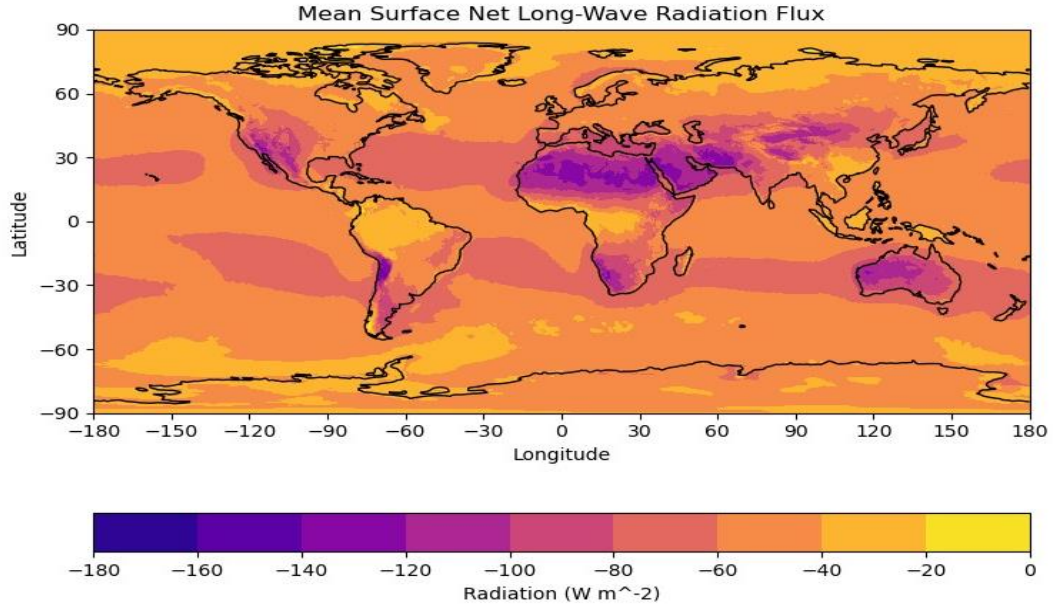


Figure 4.1.2 Decadal Global Variation of Mean Surface Net Long-wave Radiation Flux from year 2012-2023

The contour plot in figure 4.1 b shows the mean surface net longwave radiation flux over the globe for the years 2012 to 2023. Net longwave radiation flux is the difference between the upward longwave radiation emitted by the Earth's surface and the downward longwave radiation from the atmosphere. It is an important component of the Earth's energy balance.

The negative and positive signs on the latitude and longitude indicate the direction from the Equator and the Prime Meridian, respectively. Latitudes are negative in the Southern Hemisphere and positive in the Northern Hemisphere. Longitudes are negative to the west of the Prime Meridian, which runs through Greenwich, London, and positive to the east.

The scale at the bottom of the plot indicates the net longwave radiation flux in Watts per square meter (W m^2). The values range from -180 W m^2 to 0 W m^2 . The colour gradient from purple to yellow represents increasing values of radiation flux, with purple indicating the most negative values (highest net emission of longwave radiation from the surface) values ranges from -180 to -80 W m^2 and yellow indicating values closer to zero (lower net emission or more balance between emission and absorption) value ranges from -80 to 0 W m^2

Figure 4.1.1 and 4.1.2 contour plots represents different aspects of Earth's radiation balance. Shortwave radiation from the Sun provides the energy that drives Earth's climate system, while longwave radiation flux represents the exchange of heat between the Earth's surface and the atmosphere, influenced by factors such as temperature, greenhouse gases, and atmospheric conditions. Together, they regulate Earth's energy balance and play a fundamental role in shaping global climate patterns. The fig 4.1 a shows solar radiation, while the fig 4.1 b plot displays net longwave radiation flux. Solar radiation values are much higher (in the order of 10^7 J m^2) compared to net longwave radiation flux (in the order of W m^2). Solar radiation is highest near the equator and decreases towards the poles, reflecting the distribution of incoming sunlight. Net longwave radiation flux varies globally, influenced by factors like surface temperature and atmospheric composition. Both plots use colour gradients to represent radiation values, with darker shades indicating higher values. However, the scales and units differ between the two plots.

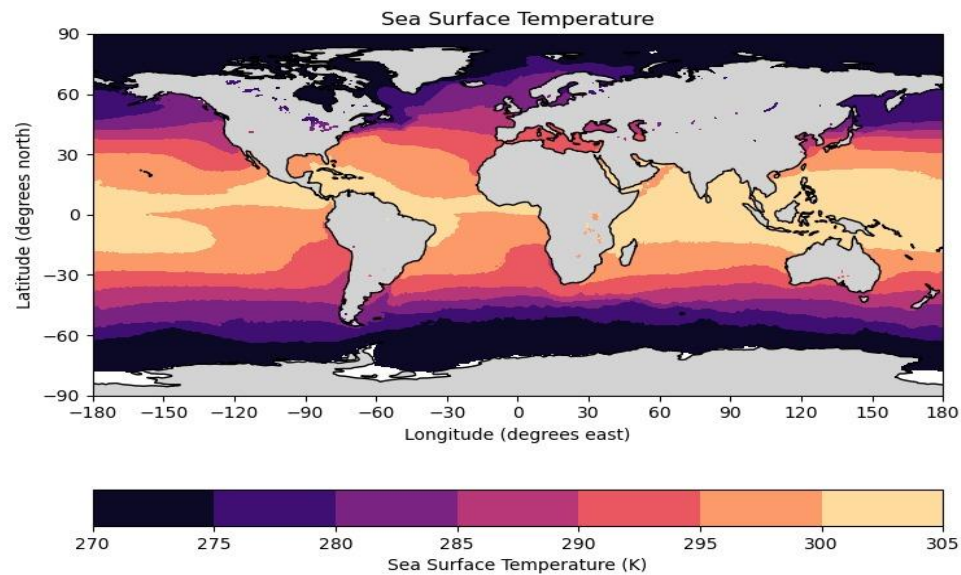


Figure 4.1.3 Decadal Global Variation of Sea Surface Temperature (SST) from year 2012-2023

The contour plot of figure 4.1.3 represents the sea surface temperature across the globe. The colours on the map correspond to different temperature ranges in Kelvin (K), as indicated by the scale at the bottom of the image. The scale ranges from 270 K, which is a colder temperature represented by the purple colour, to 305 K, which is a warmer temperature represented by the red colour.

The latitude and longitude lines are marked with both positive and negative values. Latitude values are positive in the Northern Hemisphere and negative in the Southern Hemisphere, reflecting their position relative to the equator (0 degrees latitude). Longitude values are positive to the east of the Prime Meridian (0 degrees longitude) and negative to the west. This is a standard convention for geographic coordinates.

From the contour plot, we can observe that the equatorial regions have the highest sea surface temperatures, as indicated by the shades of red and orange values ranges from

300K TO 305K. The poles, on the other hand, have the lowest temperatures, as indicated by the purple colour values ranges from 270K TO 275K. This is consistent with the general understanding that equatorial regions receive more direct sunlight and are therefore warmer, while the poles receive less sunlight and are colder. Whereas in the tropical region and subtropical there is moderate sea surface temperature values ranges from 275K TO 300K. The highest value on the scale is 305 K, and the lowest is 270 K. These values help us understand the range of sea surface temperatures across the planet.

4.2 Monthly variation in the Indian Ocean (1972-2023)

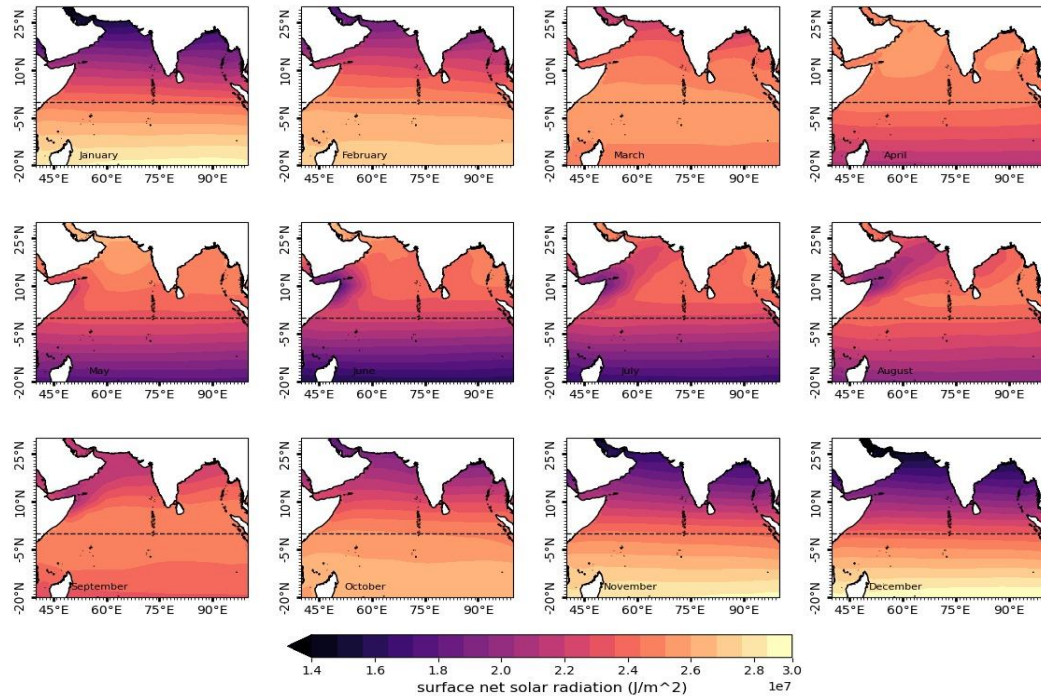


Figure 4.2.1 Monthly Variation of Surface Net Solar Radiation in the Indian Ocean
(1972-2023)

Figure 4.2.1, is a set of twelve plots, each representing the monthly variation in surface net solar radiation over the Indian Ocean for different months of the year from 1972-2023. The plots are colour-coded to indicate the amount of solar radiation received.

The scale at the bottom of the plot shows the range of surface net solar radiation values, measured in joules per square meter (J/m^2), with the values ranging from 1.4×10^7 to $3.0 \times 10^7 \text{ J/m}^2$. The colour gradient goes from purple (lower values) to orange-yellow (higher values).

The solar radiation patterns for each month based on the colour gradients are:

In month of January we observe, higher solar radiation values are observed in the southern part of the Indian Ocean, with the highest values which ranges from 2.6×10^7 to $3.0 \times 10^7 \text{ J/m}^2$ near the Tropic of Capricorn, which is consistent with the southern hemisphere's summer. Whereas it is moderate near the equator and lower solar radiation are observed in northern part of Indian Ocean in Persian Gulf and Gulf of Oman values ranging from 1.4×10^7 to $1.6 \times 10^7 \text{ J/m}^2$ and 1.6×10^7 to $2.2 \times 10^7 \text{ J/m}^2$ value ranges in Arabian Sea and Bay of Bengal. February also observed a similar variation with high values still present in the southern part, although there might be a slight decrease as the sun starts moving northward. In the month of March, the high solar radiation zone begins to shift northward, reflecting the transition from the southern hemisphere's summer to autumn. The value ranges from 2.2×10^7 to $3.0 \times 10^7 \text{ J/m}^2$. In the month of April, the high solar radiation values continue to move north, with equatorial regions receiving more intense solar radiation. And in the southern part towards downward of Indian Ocean there is slight increase in solar radiation values ranging from 2.0×10^7 to $2.2 \times 10^7 \text{ J/m}^2$. In the month of May, the northern part of the Indian Ocean starts to receive higher solar radiation values ranging from 2.2×10^7 to $2.8 \times 10^7 \text{ J/m}^2$ indicating the approach of summer in the northern hemisphere and in southern part there is increase in solar radiation values ranging from 2.4×10^7 to $1.6 \times 10^7 \text{ J/m}^2$. In month of June, the highest solar radiation values are now concentrated in the northern part of the Indian Ocean, near the Tropic of Cancer, which is consistent with the northern hemisphere's summer solstice, and in Gulf of Aden there is decrease in solar radiation vaules ranging from 2.0×10^7 to $1.8 \times 10^7 \text{ J/m}^2$. And solar radiation decreases in the

southern part near the Tropic of Capricorn. In month of July, the pattern in July is similar to June, with high solar radiation values in the northern part of the Indian Ocean. In the month of August, the high solar radiation values remain in the northern part, although there might be a slight southward shift as the sun starts moving towards the equator and slightly decreases in southern part values ranging from 2.2×10^7 to 1.8×10^7 J/m².

In month of September, the high solar radiation zone begins to shift southward, with equatorial regions receiving more intense solar radiation. And slightly decrease in solar radiation towards northward. In month of October, the solar radiation values start to increase again in the southern part of the Indian Ocean as the sun moves further south and slightly increasing towards the north.

In month of November, the southern hemisphere continues to receive higher solar radiation values, with the highest values shifting further south. Solar radiation is moderate at the equator and increases towards the north, higher solar radiation is observed in Arabian Sea and Bay of Bengal. In the month of December, the southern part of the Indian Ocean receives the highest solar radiation values ranging from 2.2×10^7 to 1.4×10^7 J/m². Solar radiation is moderate at equator and corresponding to the southern hemisphere's summer values ranging from 2.4×10^7 to 3.0×10^7 J/m².

From the monthly observations, the distribution of solar radiation in the Indian Ocean throughout the year from 1972-2023 are as follows:

There is a clear seasonal variability in solar radiation, with higher values observed during the respective hemisphere's summer months and lower values during winter months.

Solar radiation values shift northward during the northern hemisphere's summer (from May to August) and southward during the southern hemisphere's summer (from November to February). This shift is mostly observed near the Tropics of Cancer and Capricorn.

Solar radiation values are moderate around the equator throughout the year, with a slight increase as the sun approaches during the equinoxes.

There are regional differences in solar radiation values, with higher values typically observed in the open ocean compared to coastal areas or enclosed seas like the Persian Gulf and Gulf of Oman.

The distribution of solar radiation values aligns well with the seasons in each hemisphere, with higher values corresponding to summer months and lower values corresponding to winter months.

Overall, the data suggests a dynamic pattern of solar radiation distribution in the Indian Ocean, influenced by seasonal changes and geographical factors, with a clear north-south shift in response to the changing position of the sun relative to the Earth's equator.

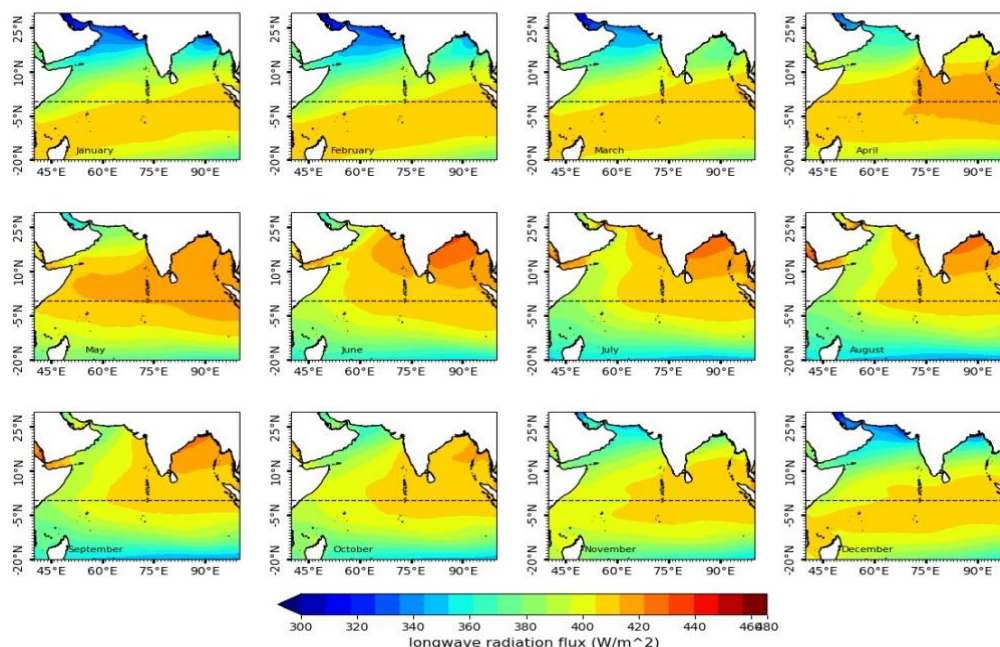


Figure 4.2.2 Monthly Variation of Mean Surface Net Long-wave Radiation Flux in the Indian Ocean (1972-2023)

Figure 4.2.2, is a plot showing longwave radiation flux values for different months of the year from 1972-2023. The colour scale at the bottom of the plot indicates the range of longwave radiation flux values in watts per square meter (W/m^2). The scale ranges from 300 W/m^2 to 4680 W/m^2 , with a gradient of colours representing different values within this range. Each plot corresponds to a different month, from January to December, and shows the distribution of longwave radiation flux across Indian Ocean as follows:

In the month of January, the longwave radiation flux in January is highest in the southern part values ranging from 400 W/m^2 to 420 W/m^2 near the Tropic of Capricorn, equator and some part in north above the equator. The lowest longwave radiation is observed in northern part of Persian Gulf and Gulf of Oman values ranging from 340

W/m^2 to $300 W/m^2$. In the month of February, the longwave radiation flux exhibits patterns similar to those observed in January, with a slightly larger portion of the southern hemisphere experiencing the highest longwave radiation flux compared to January. In the month of March, the longwave radiation flux remains consistent with that of January and February. However, what distinguishes March is the expansion of the southern region experiencing higher longwave radiation compared to earlier months. In the month of April, the highest longwave radiation flux is observed in the northern part of the Andaman and Nicobar Islands, with values ranging from 420 to 430. It decreases slightly near the Tropic of Cancer and in the southern part near the Tropic of Capricorn, with values ranging from $400 W/m^2$ to $420 W/m^2$. The lowest longwave radiation flux is found in the Gulf of Persia, ranging from $330 W/m^2$ to $320 W/m^2$, while there is a slight increase observed in the Arabian Sea. In the month of May, the highest longwave radiation flux is observed in the Arabian Sea and Bay of Bengal, ranging from $410 W/m^2$ to $430 W/m^2$. Conversely, the lowest values are found in the Gulf of Persia, with a value of $360 W/m^2$.

In the month of June, the highest longwave radiation flux is found in the northern part of the Bay of Bengal, ranging from $410 W/m^2$ to $440 W/m^2$. This flux gradually decreases towards the southern part, with values ranging from $400 W/m^2$ to $350 W/m^2$. In the month of July, the longwave radiation flux peaks in the northern regions, including the Bay of Bengal and the Gulf of Aden, gradually diminishing towards the south with values ranging between $430 W/m^2$ to $340 W/m^2$. The longwave radiation flux in August exhibits similar patterns to those observed in July. It reaches its peak in the Red Sea, with a value of $430 W/m^2$, Bay of Bengal value ranging from $440 W/m^2$ to 420

W/m^2 and gradually decreases towards the Gulf of Aden and the southern regions. In both September and October, the longwave radiation flux follows a similar pattern, with the highest values observed in the northern regions and decreasing as we move towards the southern areas. The values range from 440 W/m^2 to 340 W/m^2 . In the month of November, the longwave radiation flux is at its peak in the Bay of Bengal, gradually diminishing as we move upwards, with values ranging from 430 W/m^2 to 370 W/m^2 . Similarly, the radiation decreases towards the Arabian Sea, with values ranging from 410 W/m^2 to 360 W/m^2 , and further southward, ranging from 420 W/m^2 to 360 W/m^2 . And in the month of December, the longwave radiation flux is highest in the northern regions, particularly in the Bay of Bengal, where it peaks and gradually decreases upwards, ranging from 410 W/m^2 to 340 W/m^2 . Similarly, in the Arabian Sea, the radiation is higher near the equator and diminishes as it moves northward, with values ranging from 410 W/m^2 to 300 W/m^2 . In the southern part, the radiation is highest at the equator and decreases towards the south, ranging from 410 W/m^2 to 380 W/m^2 .

Based on the observations from January to December over the years 1972 to 2023

There are clear seasonal variations in the longwave radiation flux across the studied regions, with the flux typically peaking in the southern hemisphere during the local summer months (December to February) and in the northern hemisphere during the local summer months (June to August). The distribution of longwave radiation flux varies across different regions, with some areas consistently experiencing higher flux values (e.g., Bay of Bengal, Arabian Sea) compared to others (e.g., Gulf of Persia, Gulf of Oman).

There is a noticeable latitudinal influence on the longwave radiation flux, with higher values typically observed nearer to the equator and decreasing towards the poles. Despite some fluctuations, there appears to be a general consistency and trend in the observed patterns over the years, with similar seasonal variations and geographical distributions observed annually.

While the overall patterns remain consistent, there may be some interannual variability in the specific values and extents of longwave radiation flux, which could be influenced by factors such as climate variability and atmospheric conditions. Certain regions, such as the Bay of Bengal and the Arabian Sea, consistently exhibit higher longwave radiation flux throughout the year, suggesting unique regional dynamics and influences on the radiation balance. The presence of specific oceanic features (e.g., Andaman and Nicobar Islands, Red Sea) and atmospheric conditions likely play a significant role in shaping the distribution and intensity of longwave radiation flux in the studied regions.

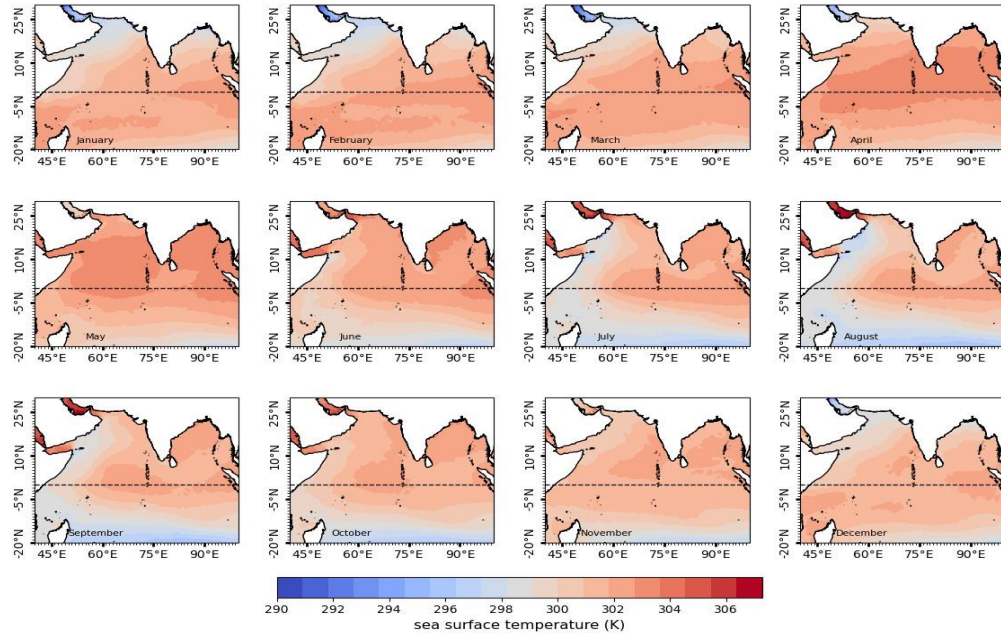


Figure 4.2.3 Monthly Variation of Sea Surface Temperature (SST) in the Indian Ocean
(1972-2023)

Figure 4.2.3, is a set of monthly sea surface temperature (SST) plots for the Indian Ocean, from year 1972 to 2023 covering the months from January to December. Each plot represents the spatial distribution of SSTs for a specific month. The temperatures are given in Kelvin (K), which is an absolute temperature scale.

The scale at the bottom of the plot indicates the range of temperatures displayed on the plots, with the colour gradient representing different temperatures. The scale goes from 290 K (which is about 16.85°C) to 306 K (which is about 32.85°C). The warmer temperatures are typically represented by the redder colours, while cooler temperatures are represented by the bluer colours.

From the plots, we can observe the following general patterns:

- The northern hemisphere of the Indian Ocean tends to be warmer during the northern hemisphere's summer months (June, July, August) and cooler during its winter months (December, January, February).
- Conversely, the southern hemisphere of the Indian Ocean shows warmer temperatures during the southern hemisphere's summer months (December, January, February) and cooler temperatures during its winter months (June, July, August).
- The equatorial region generally remains warm throughout the year, with less pronounced seasonal variation compared to the northern and southern extremes.

Regarding solar radiation, it is not directly shown on these plots, but it is a primary factor influencing sea surface temperatures. Generally, solar radiation is more intense during the summer months for each hemisphere, leading to warmer sea surface temperatures. During winter, the angle of solar incidence is lower, and days are shorter, leading to less solar radiation and cooler sea surface temperatures.

From the observation from year 1972 to 2023 for each month, Sea surface temperatures in the Indian Ocean exhibit significant seasonal variation in both the northern and southern hemispheres. This variation is primarily driven by the changing intensity and angle of solar radiation throughout the year.

There is a clear contrast between the seasonal patterns of sea surface temperatures in the northern and southern hemispheres of the Indian Ocean. During the summer months in one hemisphere, the opposite hemisphere experiences its winter, leading to contrasting temperature pattern.

The equatorial region of the Indian Ocean experiences relatively stable and warm temperatures throughout the year compared to the more variable temperatures seen in the northern and southern extremes. This is because the equatorial region receives relatively consistent solar radiation year-round due to its proximity to the equator.

Solar radiation plays a crucial role in driving the seasonal variation in sea surface temperatures. Higher solar radiation during the summer months leads to warmer temperatures, while lower solar radiation during winter results in cooler temperatures.

From the observations of figures 4.2.1, 4.2.2, 4.2.3;

There is a clear seasonal variability in solar radiation across the Indian Ocean, with higher values during each hemisphere's summer months and lower values during winter months. This variation aligns well with the observed seasonal patterns in sea surface temperatures.

Solar radiation values exhibit a northward shift during the northern hemisphere's summer and a southward shift during the southern hemisphere's summer, primarily near the Tropics of Cancer and Capricorn. This shift corresponds to changes in the position of the sun relative to the Earth's equator.

Similar to solar radiation, there are regional differences in longwave radiation flux across different areas of the Indian Ocean. Some regions consistently experience higher flux values, particularly near the equator and in certain oceanic features such as the Bay of Bengal and the Arabian Sea.

The observed seasonal variation in sea surface temperatures is primarily driven by changes in solar radiation intensity and angle throughout the year. Higher solar radiation

during summer months leads to warmer sea surface temperatures, while lower radiation during winter months results in cooler temperatures.

The equatorial region of the Indian Ocean exhibits relatively stable and warm temperatures throughout the year due to its proximity to the equator and consistent solar radiation. This stability contrasts with the more variable temperatures observed in the northern and southern extremes.

Overall, these observations highlight the interconnected relationship between solar radiation, longwave radiation flux, and sea surface temperatures in the Indian Ocean, with seasonal variations and regional differences playing significant roles in shaping the oceanic climate dynamics.

4.3 Global Time Series Plot: Anomalies in Climate Data (1972-2023).

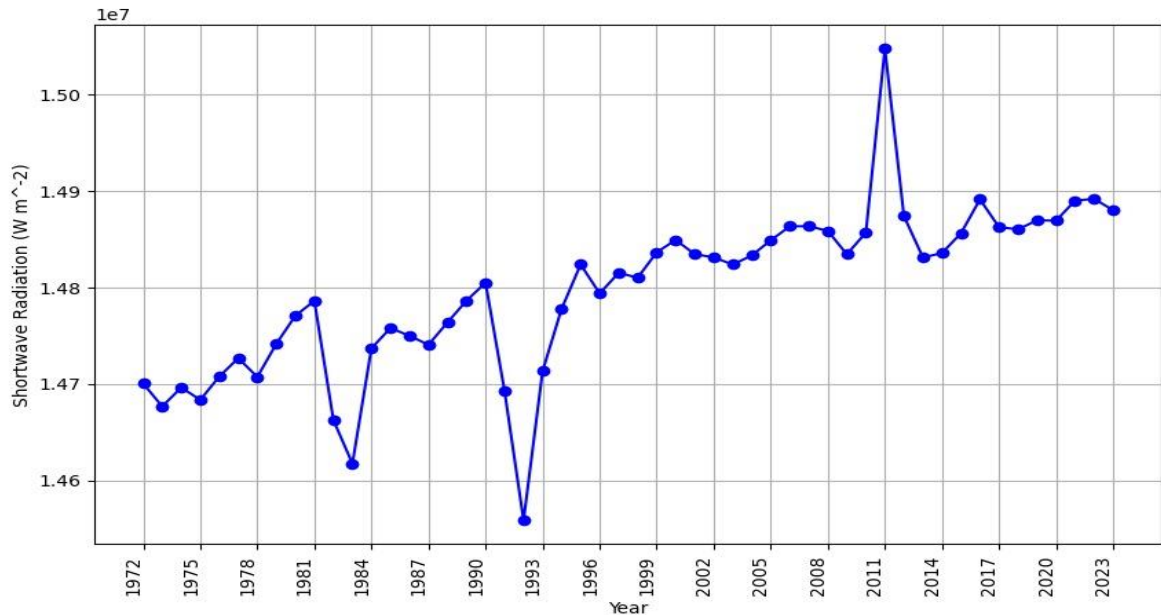


Figure 4.3.1 Time series plot of Surface Net Shortwave Solar Radiation from year 1972-2023

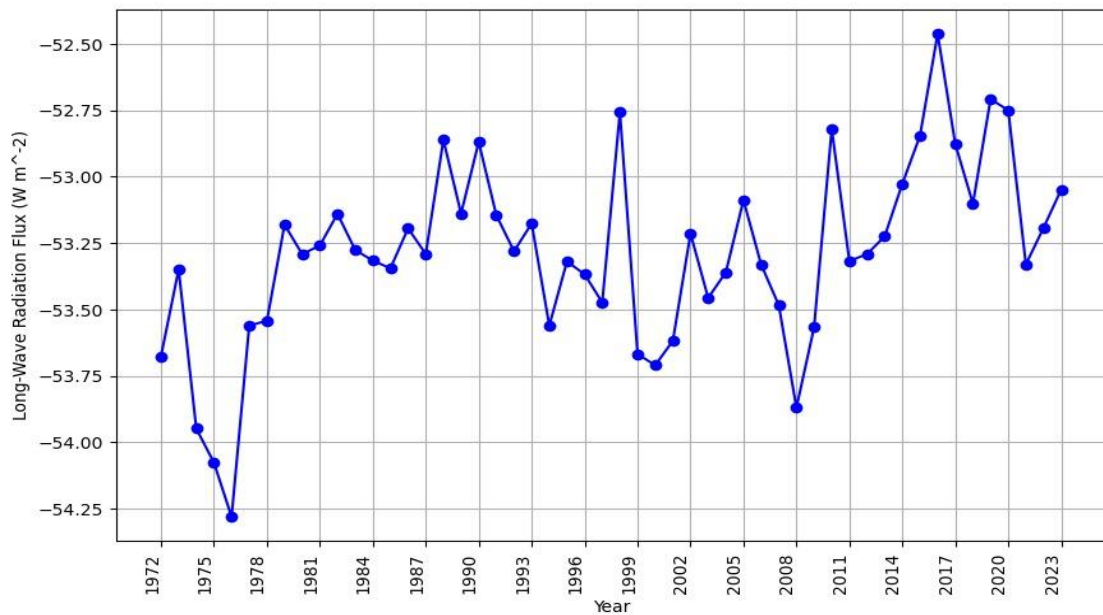
Figure 4.3.1, is a time series plot of global surface net shortwave solar radiation from the year 1972 to 2023. The y-axis represents the shortwave radiation in watts per square meter (W/m^2), and the x-axis represents the years.

The scale on the y-axis ranges from $1.46 \times 10^7 \text{ W}/\text{m}^2$ to $1.50 \times 10^7 \text{ W}/\text{m}^2$. The plot uses a line graph with data points marked by dots to show the annual variation in solar radiation.

From the plot, we can observe that, there is a general fluctuation in the amount of solar radiation from year to year, with no clear long-term trend of increase or decrease over the entire period.

There are some notable dips in the radiation levels at certain points, such as around the mid-1980s, the early 1990s, and the early 2010s. These could be due to various factors, including volcanic activity, which can inject aerosols into the atmosphere and reduce the amount of sunlight reaching the Earth's surface.

There is a significant spike in radiation around the year 2020. It could be due to unusual environmental event, or other factors affecting global solar radiation. The variation from year to year seems to be within a range of about $0.04 \times 10^7 \text{ W/m}^2$, which is relatively small, compared to the overall values.



4.3.2 Time series plot of Mean Surface Net Longwave Radiation Flux from year 1972-2023

The figure 4.3.2, is a time series plot of the global mean surface net longwave radiation flux, measured in watts per square meter (W/m^2), from the year 1972 to 2023. The y-axis of the plot represents the longwave radiation flux values, which range from $54.25 \text{ W}/\text{m}^2$ to $-52.50 \text{ W}/\text{m}^2$. The x-axis represents time, with each point corresponding to a year from 1972 to 2023.

The negative sign in front of the values indicates that this is a net outgoing longwave radiation flux. This means that the amount of longwave radiation leaving the Earth's surface (emitted by the surface) is greater than the amount coming in (downwelling longwave radiation from the atmosphere). It's a convention in Earth's energy budget studies to consider outgoing energy as negative because it represents a loss of energy from the surface.

The plot shows fluctuations in the mean surface net longwave radiation flux over the years. There are peaks and troughs indicating that some years experienced higher net losses of longwave radiation, while others experienced lower net losses. These variations can be due to several factors, including changes in surface temperature, cloud cover, atmospheric water vapour, and concentrations of other greenhouse gases, which all affect the longwave radiation balance.

In figure 4.3.1 and 4.3.2, time series plots of global surface net shortwave solar radiation and global mean surface net longwave radiation flux plots depict fluctuations in radiation flux over time, they represent different components of Earth's energy budget. Solar radiation represents incoming energy from the Sun, while longwave radiation flux represents outgoing energy emitted by the Earth's surface. The fluctuations observed in both plots reflect natural variability and potential influences from external factors such as volcanic activity or environmental events. Additionally, variations in longwave radiation flux are influenced by surface temperature and atmospheric conditions, highlighting the complex interplay of factors shaping Earth's radiation balance.

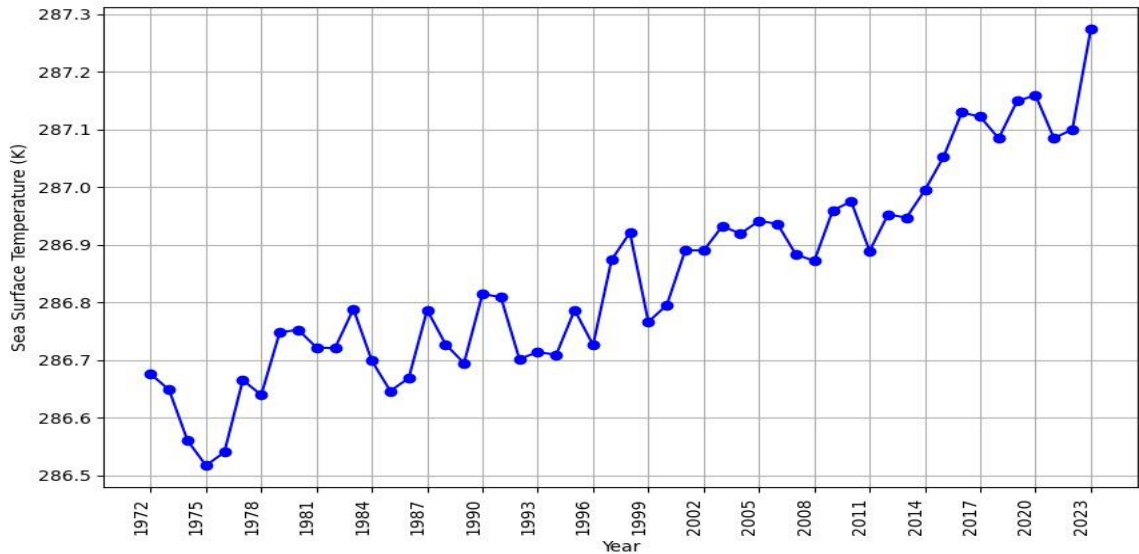


Figure 4.3.3 Time series plot of Sea Surface Temperature (SST) from year 1972-2023

Fig. 4.3.3 is a time series plot of the global mean sea surface temperature (SST) from the year 1972 to 2023, measured in Kelvin (K). The y-axis of the plot represents the sea surface temperature values, which range from about 286.5 K to 287.3 K. The x-axis represents time, with each point corresponding to a year from 1972 to 2023. The plot shows fluctuations in the mean sea surface temperature over the years. The data points, represented by dots, are connected by lines, which helps to visualize the trend and variability over time. There are peaks and troughs indicating that some years experienced higher temperatures, while others experienced lower temperatures.

From the plot, we can observe that there is a general upward trend in the sea surface temperature over the 50-year period. The early years show lower temperatures, with some variability, and starting from around the mid-1990s, there is a more pronounced increase in temperature, reaching its highest values towards the end of the time series. This upward trend is consistent with the general scientific understanding that global

temperatures have been rising, which is often associated with global warming due to increased greenhouse gas concentrations in the atmosphere. The variability from year to year can be influenced by a variety of factors, including natural climate variability like El Niño and La Niña events, volcanic activity, solar radiation changes, and anthropogenic factors such as greenhouse gas emissions and land use changes.

4.4 DISCUSSION

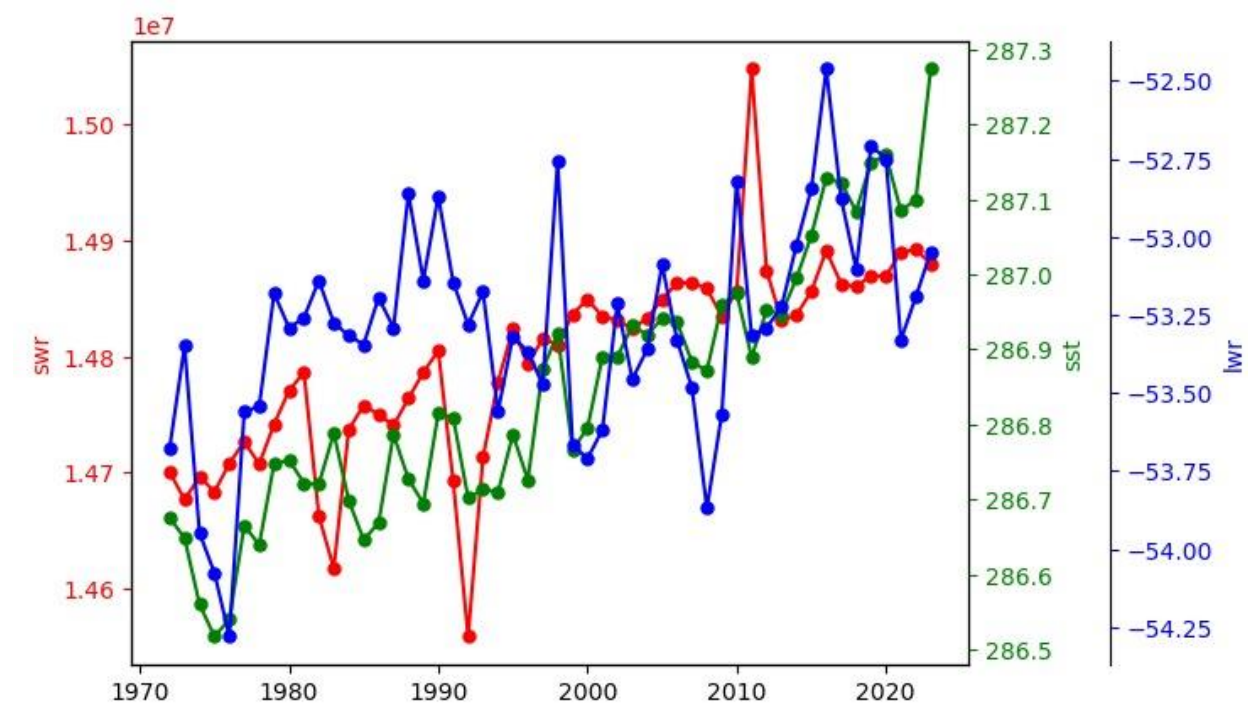


Figure 4.4.1 Temporal Trends: Shortwave Radiation, Longwave Radiation, and Sea Surface Temperature over Year (1972-2023)

Figure 4.4.1, is a plot that illustrates how shortwave radiation, longwave radiation, and sea surface temperature have changed over the span of 51 years, from 1972 to 2023. This plot likely shows the trends, patterns, and possible relationships between these variables over time, providing insights into the dynamics of Earth's climate system. Over the past 50 years, each dot on the graph represents a year. The shortwave radiation line, depicted in red, fluctuates between values of $1.46 \times 10^7 \text{ J m}^{-2}$ to $1.50 \times 10^7 \text{ J m}^{-2}$. The longwave radiation line, shown in blue, ranges from -52.50 W m^{-2} to -54.25 W m^{-2} . Meanwhile, the sea surface temperature line, illustrated in green varies between the ranges 286.5K to 287.3K . Notably, the shortwave radiation line

demonstrates a drop in radiation levels in the year 1992. The decrease in shortwave radiation could be due to various factors, including natural phenomena and anthropogenic activities.

Potential reasons for a decrease in shortwave radiation during that year might include:

- Major volcanic eruptions can inject large amounts of ash and sulfur dioxide into the atmosphere, which can reflect sunlight back into space and lead to a temporary reduction in shortwave radiation reaching the Earth's surface. While the sun's output is relatively stable, there can be short-term fluctuations in solar activity, such as sunspot cycles or solar flares, which may result in slight variations in shortwave radiation received by the Earth. Changes in atmospheric composition, such as increases in aerosols or clouds, can affect the amount of shortwave radiation reaching the surface by scattering or absorbing sunlight. Shifts in weather patterns, such as increased cloud cover or atmospheric moisture content, can also influence the amount of shortwave radiation reaching the Earth's surface. While less common, changes in land use or industrial activities can also impact shortwave radiation by altering surface reflectivity or atmospheric composition.

There was highest solar radiation in year 2010 could be due to Solar radiation levels can vary due to changes in solar activity, such as fluctuations in the sunspot cycle or solar output. If 2010 experienced a period of increased solar activity, it could result in higher levels of shortwave radiation reaching the Earth's surface. Changes in atmospheric circulation patterns and weather conditions can influence the amount of sunlight reaching the Earth's surface. If 2010 had weather conditions that favoured clearer skies

and reduced cloud cover over a large area, this could have led to higher levels of shortwave radiation.

Long-term climate patterns, such as El Niño or La Niña events, can affect regional and global weather patterns, including cloud cover and atmospheric circulation. Changes in these patterns could contribute to variations in shortwave radiation levels. Events such as wildfires or volcanic eruptions can release aerosols and particulate matter into the atmosphere, which can affect the scattering and absorption of sunlight, potentially leading to short-term fluctuations in shortwave radiation levels. While less significant than natural factors, human activities such as changes in land use, urbanization, and industrial emissions can also influence shortwave radiation levels, although typically to a lesser extent compared to natural factors.

The fluctuation in the longwave radiation line displays variations in outgoing longwave radiation, indicated by negative values. In 1976, there was a notable increase in longwave radiation, whereas in 2016, it decreased. These changes can occur due to various factors. Changes in the composition of the atmosphere, such as variations in greenhouse gas concentrations (e.g., carbon dioxide, water vapour, methane), can influence the absorption and emission of longwave radiation. For example, increased concentrations of greenhouse gases enhance the greenhouse effect, leading to higher longwave radiation levels.

Clouds play a crucial role in the Earth's radiation budget. Depending on their altitude, thickness, and composition, clouds can either absorb or reflect longwave radiation. Therefore, changes in cloud cover can result in fluctuations in longwave radiation

reaching the Earth's surface. Water vapour is a potent greenhouse gas and plays a significant role in the absorption and emission of longwave radiation in the atmosphere. Changes in atmospheric water vapour content due to evaporation, condensation, or atmospheric circulation patterns can impact longwave radiation levels. Variations in incoming solar radiation (shortwave radiation) can indirectly affect longwave radiation levels by altering surface temperatures and atmospheric conditions. For example, changes in solar activity or orbital parameters can lead to fluctuations in surface temperatures and atmospheric dynamics, consequently impacting longwave radiation.

The sea surface temperature (SST) trend indicates a steady increase over the years, with the lowest recorded in 1975 and the highest in 2023. This upward trend in SST from 1972 to 2023 can be attributed to various factors. The increase in atmospheric concentrations of greenhouse gases, such as carbon dioxide (CO₂), methane (CH₄), and nitrous oxide (N₂O), due to human activities like burning fossil fuels, deforestation, and industrial processes, has led to enhanced trapping of outgoing longwave radiation. This phenomenon, known as the greenhouse effect, has resulted in warming of the Earth's surface and oceans, including SST.

The oceans act as a vast reservoir of heat and absorb a significant portion of the excess heat trapped by greenhouse gases in the atmosphere. This process, known as ocean heat uptake, contributes to the warming of SST over time. Warmer temperatures cause seawater to expand thermally, leading to an increase in sea level. This thermal expansion contributes to the observed rise in SST, as warmer waters occupy a larger volume. Alterations in ocean circulation patterns, such as shifts in currents,

upwelling/downwelling processes, and the strength and location of major ocean currents like the Gulf Stream, can influence SST regionally and globally.

The opposite trends observed in the shortwave radiation line and longwave radiation line can be explained by the interconnected processes of the Earth's energy balance. An increase in shortwave radiation, typically from incoming solar radiation, can trigger certain effects within the Earth's atmosphere and surface. These effects may lead to changes that ultimately result in a decrease in longwave radiation, which primarily represents outgoing thermal radiation from the Earth. During periods of clear skies with minimal cloud cover, more shortwave radiation reaches the Earth's surface, leading to higher levels of incoming solar radiation. However, with fewer clouds to trap and emit longwave radiation, there might be a relative decrease in longwave radiation emitted from the atmosphere. In regions with low atmospheric humidity, there is less water vapour to absorb and emit longwave radiation. Consequently, an increase in shortwave radiation may not be fully compensated by an increase in longwave radiation emitted by the atmosphere, resulting in a net decrease in longwave radiation. Increased shortwave radiation can lead to heating of the Earth's surface, causing it to emit more longwave radiation upward. However, if the atmosphere above the surface is opaque to certain wavelengths of longwave radiation (for instance, due to the presence of greenhouse gases), some of this emitted radiation may be absorbed and re-emitted back towards the surface, reducing the overall amount of longwave radiation escaping to space.

There is a correlation between longwave radiation and sea surface temperature. When longwave radiation increases, it can contribute to an increase in sea surface temperature. This relationship is due to the fact that longwave radiation, which represents the

outgoing thermal radiation emitted by the Earth, is absorbed by the ocean surface, leading to a rise in temperature. Longwave radiation, also known as infrared radiation, is emitted by the Earth's surface, including the ocean, as heat. When longwave radiation is absorbed by the ocean's surface, it contributes to heating the water, thus potentially increasing SST. The absorption and re-emission of longwave radiation by greenhouse gases in the atmosphere can influence SST. Greenhouse gases trap some of the longwave radiation emitted by the Earth's surface, including the oceans, leading to warming of the atmosphere. This can result in a warmer atmospheric layer above the ocean, which may in turn affect SST through various mechanisms such as altered heat exchange between the atmosphere and ocean. The relationship between shortwave radiation (incoming solar radiation), longwave radiation (outgoing terrestrial radiation), and sea surface temperature (SST) is fundamental to understanding the Earth's energy balance.

Changes in SST can influence both shortwave and longwave radiation through feedback mechanisms. For example, warmer SST can enhance evaporation rates, leading to increased atmospheric humidity. This higher humidity can affect the absorption and scattering of both shortwave and longwave radiation in the atmosphere. Additionally, changes in SST can influence cloud cover and atmospheric circulation patterns, which can further impact the distribution of incoming solar radiation and the emission of outgoing terrestrial radiation.

4.5 CONCLUSION:

The Earth's heat budget refers to the balance between the incoming and outgoing energy fluxes that maintain the Earth's temperature equilibrium. It involves various processes, including incoming solar radiation, outgoing longwave radiation, atmospheric absorption and reflection, and heat transfer between the Earth's surface and atmosphere.

The observations from the contour plots of figure 4.1 highlight the intricate relationships between solar radiation distribution, net longwave radiation flux, and sea surface temperature, all of which play pivotal roles in shaping the Earth's heat budget.

Solar radiation serves as the primary energy input into the Earth's climate system, influencing temperature patterns and driving atmospheric circulation. The distribution of solar radiation across the globe dictates regional temperature variations, with equatorial regions receiving more radiation and experiencing warmer temperatures, while Polar Regions receive less radiation and are colder.

Net longwave radiation flux represents the balance between incoming and outgoing thermal radiation at the Earth's surface, encompassing absorption and emission processes. Higher temperatures lead to increased emission of longwave radiation, contributing to a positive net flux, whereas colder regions emit less radiation, resulting in a negative net flux. Various factors such as cloud cover, greenhouse gas concentrations, and surface properties influence the distribution of net longwave radiation flux.

Sea surface temperature reflects the thermal state of the ocean, acting as a reservoir of heat and being influenced by solar radiation, ocean currents, and atmospheric

circulation. The redistribution of heat through oceanic circulation patterns affects global climate dynamics, with warmer temperatures near the equator and cooler temperatures towards the poles.

Solar radiation drives temperature variations, which, in turn, influence sea surface temperature patterns. Changes in sea surface temperature impact the emission and absorption of longwave radiation, thereby contributing to variations in the net longwave radiation flux.

From the figures 4.1.1, 4.1.2 and 4.1.3 contour plots representing solar radiation distribution, net longwave radiation flux, and sea surface temperature. There are consistent spatial patterns observed across all three plots. Warmer temperatures and higher solar radiation levels are concentrated around the equator, while colder temperatures and lower radiation levels are found towards the poles. This demonstrates the influence of latitude on climate variables due to the Earth's spherical shape and axial tilt.

Each plot represents a different aspect of Earth's climate system. Despite representing different variables, there are interconnected processes. For example, solar radiation drives temperature variations across the globe, influencing sea surface temperature patterns. Additionally, variations in temperature can affect the emission and absorption of longwave radiation, contributing to the net longwave radiation flux.

The plots collectively highlight the complexity of global climate patterns and the interplay of various factors in shaping Earth's climate. Factors such as latitude, land-sea distribution, ocean currents, atmospheric circulation, and greenhouse gas concentrations

all contribute to the observed spatial patterns in solar radiation, longwave radiation flux, and temperature.

Figure 4.2 shows the significant seasonal variability observed in solar radiation, longwave radiation flux, and sea surface temperature across the Indian Ocean.

Solar radiation exhibits distinct seasonal patterns, with higher values during each hemisphere's summer months and lower values during winter months. This variability aligns closely with observed patterns in sea surface temperatures, highlighting the strong relationship between solar radiation and oceanic temperature dynamics. Additionally, there is a noticeable northward shift in solar radiation during the northern hemisphere's summer and a southward shift during the southern hemisphere's summer, particularly near the Tropics of Cancer and Capricorn. These shifts correspond to changes in the sun's position relative to the Earth's equator, influencing regional climate patterns.

Similarly, longwave radiation flux displays regional differences across the Indian Ocean, with certain regions consistently experiencing higher flux values, notably near the equator and in specific oceanic features such as the Bay of Bengal and the Arabian Sea.

The observed seasonal variation in sea surface temperatures is primarily attributed to changes in solar radiation intensity and angle throughout the year. Higher solar radiation during summer months contributes to warmer sea surface temperatures, while lower radiation during winter months results in cooler temperatures. Notably, the equatorial region of the Indian Ocean maintains relatively stable and warm temperatures year-

round due to its proximity to the equator and consistent solar radiation, contrasting with the more variable temperatures observed in the northern and southern extremes.

And from figure 4.3 Time series plot from year 1972-2023 of 4.3.1 Surface net shortwave solar radiation, 4.3.2 mean surface net longwave radiation flux and 4.3.3 sea surface temperature, the conclusion of this plots are as follows:

Solar radiation, longwave radiation flux, and sea surface temperature are interconnected components of Earth's energy balance and climate system. Changes in solar radiation, both incoming shortwave and outgoing longwave, play a crucial role in driving variations in surface temperature and sea surface temperature (SST).

In conclusion, the time series plots presented in Figure 4.3 illustrate the interconnected nature of solar radiation, longwave radiation flux, and sea surface temperature, all fundamental components of Earth's energy balance and climate system.

Variations in solar radiation, encompassing both incoming shortwave and outgoing longwave radiation, serve as key drivers of fluctuations in surface temperature and sea surface temperature (SST). These changes in solar radiation intensity directly influence temperature patterns, highlighting their significant impact on Earth's climate dynamics.

The conclusion drawn from Figure 4.4.1 indicates that with an increase in incoming solar radiation, there is a corresponding rise in sea surface temperature. This increase in shortwave radiation results in a decrease in longwave radiation. The reason for this observed trend is related to the Earth's energy balance. When there is an increase in incoming solar radiation (shortwave radiation), more energy is absorbed by the Earth's surface and ocean. This absorbed energy then leads to a rise in temperature, including

the temperature of the sea surface. As the temperature increases, the Earth emits more longwave radiation (outgoing thermal radiation) to balance the incoming energy. However, since the increase in shortwave radiation contributes to warming, the increase in longwave radiation is not sufficient to offset this warming effect entirely. Therefore, despite an increase in longwave radiation, the net effect is a rise in sea surface temperature.

REFERENCES

1. Alexandrov, M. D., Cairns, B., Emde, C., Ackerman, A. S., & van Diedenhoven, B. (2012). Accuracy assessments of cloud droplet size retrievals from polarized reflectance measurements by the research scanning polarimeter. *Remote Sensing of Environment*, 125, 92-111.
2. Abraham, J. P., Baringer, M., Bindoff, N. L., Boyer, T., Cheng, L. J., Church, J. A., & Willis, J. K. (2013). A review of global ocean temperature observations: Implications for ocean heat content estimates and climate change. *Reviews of Geophysics*, 51(3), 450-483.
3. An, Ni & Hemmati, Sahar & Cui, Yu-jun. (2017). Assessment of the methods for determining net radiation on different time-scales of meteorological variables. *Journal of Rock Mechanics and Geotechnical Engineering*. 9. 10.1016/j.jrmge.2016.10.004.
4. Chen, L., & Wang, X. (2021). Indian Ocean Warming and Its Implications for Global Climate Change. *Earth's Future*, 9(2), e2020EF001678
5. David H. Miller, H.E.Landsberg, J.Van Mieghem The Heat and Water Budget of the Earth's Surface, (2011), *Advances in Geophysics*, Elsevier, 1965,Pages 175-302,[https://doi.org/10.1016/S0065-2687\(08\)60497-5](https://doi.org/10.1016/S0065-2687(08)60497-5).
6. Drakakis, Emmanuel Hatzidimitriou, Despina Vardavas, I. (2005). Global distribution of Earth's surface shortwave radiation budget. *Atmospheric Chemistry and Physics*. 5. 2847-2867. 10.5194/acpd-5-4545-2005.

7. Donlon, C. J., Martin, M., Stark, J., Roberts-Jones, J., Fiedler, E., & Wimmer, W. (2012). The Operational Sea Surface Temperature and Sea Ice Analysis (OSTIA) system. *Remote Sensing of Environment*, 116, 140-158.
8. Das, S., & Mukherjee, A. (2020). Variability of Heat Fluxes Between the Indian Ocean and Atmosphere: Observations and Mechanisms. *Journal of Climate*, 33(10), 4205-4223.
9. Emery, W. J., & Meincke, J. (1986). Global sea surface temperature and its relation to atmospheric forcing fields. *Journal of Geophysical Research: Oceans*, 91(C7), 8411-8425.
10. Ebtehaj, I., Soltani, K., Amiri, A., Faramarzi, M., Madramootoo, C. A., & Bonakdari, H. (2021). Prognostication of shortwave radiation using an improved no-tuned fast machine learning. **Sustainability*, 13*, 8009. <https://doi.org/10.3390/su13148009>
11. Gil, s., Mayo chi, m.Pelisse, l. j. (2006). experimental estimation of the luminosity of the sun. *American journal of physics*, 74(8), 728–733. doi:10.1119/1.2192789.
12. Gao, Z., & Huang, X. (2011). Development of a simple algorithm to estimate the daily downward longwave radiation from MODIS data over rugged terrain. *Remote Sensing of Environment*, 115(6), 1561-1572.
13. Gaillard, F., Dushaw, B. D., Park, J. H., & Baggeroer, A. B. (2010). Interannual sea surface temperature variability in the North Atlantic and its impact on low-frequency underwater sound. *The Journal of the Acoustical Society of America*, 128(2), 637-647.

14. Gentemann, C. L., Clayson, C. A., Brown, S., Lee, T., Parfitt, R., Farrar, J. T., & Bluth, R. T. (2019). Satellite sea surface temperatures along the west coast of the United States during the 2014–2016 northeast Pacific marine heat wave. *Geophysical Research Letters*, 46(14), 8395-8404.
15. Gupta, A., & Sharma, R. (2018). Indian Ocean Heat Uptake and Its Role in Modulating Global Climate Sensitivity. *Geophysical Research Letters*, 45(19), 10,610-10,618.
16. Huang, D., Zhou, L., Dickinson, R. E., & Chameides, W. L. (2007). Impact of aerosol indirect effect on surface temperature over East Asia. *Proceedings of the National Academy of Sciences*, 104(38), 14889-14894.
17. Hatzianastassiou, N. Matsoukas, Christos Fotiadi, A. Pavlakis, K. & Hatfield, Jerry Baker, J.M. Klassen, Steve Bugbee, Bruce. (2005). Shortwave Radiation. 10.2134/Agronmonogr47.C3.
18. . Hatzianastassiou, N., Matsoukas, C., Fotiadi, A., Pavlakis, K. G., Drakakis, E., Hatzidimitriou, D., & Vardavas, I. (2004). Long-term global distribution of Earth's shortwave radiation budget at the top of atmosphere. *Atmospheric Chemistry and Physics*, 4(11), 2397-2411.
19. Harries, J. E., Russell, J. E., Hanafin, J. A., Brindley, H. E., Futyran, J., Rufus, J., & Last, A. (2005). The Geostationary Earth Radiation Budget (GERB) project. *Bulletin of the American Meteorological Society*, 86(6), 945-960.
20. Huang, X., Huang, X., & Gao, Z. (2009). Development of a high spatial resolution longwave radiation product derived from MODIS surface temperature

- and spectral reflectance. *Journal of Geophysical Research: Atmospheres*, 114(D4).
21. Inamdar, Anand & Guillevin, Pierre. (2015). net surface shortwave radiation from goes imagery—product evaluation using ground-based measurements from surface and remote sensing. 7. 10788-10814.10.3390/rs70810788.
 22. Kandel, S., Becker, F., Stöckli, R., & Coll, C. (2018). Evaluation of cloud and water vapour estimates from SEVIRI versus MODIS over Europe. *Remote Sensing*, 10(3), 462.
 23. . Kato, S., Loeb, N. G., Rose, F. G., Doelling, D. R., Rutan, D. A., Caldwell, T. E., & Smith Jr, W. L. (2013). Surface irradiances consistent with CERES-derived top-of-atmosphere shortwave and longwave irradiances. *Journal of Climate*, 26(9), 2719-2740.
 24. Khan, F., & Ali, M. (2021). Indian Ocean Heat Content Trends in a Warming Climate: Observational Evidence and Future Projections. *International Journal of Climatology*, 41(1), 157-171.
 25. Kumar, M., & Singh, R. (2020). Heat Fluxes in the Indian Ocean: Observations, Models, and Implications for Climate Studies. *Journal of Geophysical Research: Oceans*, 125(8), e2019JC015790
 26. Liang, S. (2000). Narrowband to broadband conversions of land surface albedo I: Algorithms. *Remote Sensing of Environment*, 76(2), 213-238.
 27. Li, Z., Li, C., & Schmetz, J. (2006). A review of satellite remote sensing of surface solar radiation. *Remote Sensing Reviews*, 25(1-2), 5-23.

28. Liu, W. T., & Xie, X. (1999). ENSO prediction with Markov models: the impact of sea surface temperature anomalies. *Journal of Climate*, 12(10), 2851-2863.
29. Liu, G., Xie, S. P., & Liu, Q. (2016). Western Pacific emergent constraint lowers projected increase in Indian summer monsoon rainfall. *Nature Climate Change*, 6(10), 1115-1120.
30. Lee, J. H., & Kim, S. (2019). Oceanic Heat Transport in the Indian Ocean: Observations and Modeling Studies. *Journal of Physical Oceanography*, 49(6), 1529-1545.
31. Merchant, C. J., Embury, O., Roberts-Jones, J., Fiedler, E., Bulgina, C. E., Corlett, G. K., & Le Borgne, P. (2012). Sea surface temperature datasets for climate applications from phase 1 of the European Space Agency Climate Change Initiative (SST CCI). *Geoscience Data Journal*, 1(2), 179-191.
32. Nguyen, T., & Thanh, L. (2017). Heat Budget of the Indian Ocean: Observations, Models, and Uncertainties. *Ocean Dynamics*, 67(9), 1165-1181.
33. Ohmura, A., Dutton, E. G., Forgan, B., Frohlich, C., Gilgen, H., Hegner, H., & Rummukainen, M. (1998). Baseline Surface Radiation Network (BSRN/WCRP): New precision radiometry for climate research. *Bulletin of the American Meteorological Society*, 79(10), 2115-2136.
34. Pinker, R. T., Zhang, B., & Dutton, E. G. (2006). Climatic effect of clouds on surface shortwave absorption at Barrow, Alaska. *Journal of Climate*, 19(13), 3157-3170.
35. Pilewskie, P., Bergstrom, R. W., Mariani, L., Gore, W. J., Howard, S. D., & Rabbette, M. (2003). Solar spectral radiative forcing during the Southern African

- Regional Science Initiative. *Journal of Geophysical Research: Atmospheres*, 108(D13).
36. Patel, R., & Gupta, S. (2019). Indian Ocean Heat Content Changes and Their Impact on Climate Variability. *Climate Dynamics*, 52(3-4), 1621-1635.
37. Reynolds, R. W., Rayner, N. A., Smith, T. M., Stokes, D. C., & Wang, W. (2002). An improved in situ and satellite SST analysis for climate. *Journal of Climate*, 15(13), 1609-1625.
38. Ramanathan, V., Crutzen, P. J., Kiehl, J. T., & Rosenfeld, D. (2001). Aerosols, climate, and the hydrological cycle. *Science*, 294(5549), 2119-2124.
39. Rahman, S., & Ahmed, K. (2017). Interannual to Decadal Variability of Heat Content in the Indian Ocean and its Role in Modulating Global Climate. *Geophysical Research Letters*, 44(18), 9315-9323.
40. Stephens, G. L., Li, J., Wild, M., Clayson, C. A., Loeb, N., Kato, S., & Stackhouse Jr, P. W. (2012). An update on Earth's energy balance in light of the latest global observations. *Nature Geoscience*, 5(10), 691-696.
41. Smith, A. B., & Jones, C. D. (2018). Role of the Indian Ocean in Regional and Global Climate Variability. *Journal of Climate*, 31(10), 3987-4002.
42. Wild, M., Gilgen, H., Roesch, A., Ohmura, A., Long, C. N., Dutton, E. G., & McKeegan, K. (2005). From dimming to brightening: Decadal changes in solar radiation at Earth's surface. *Science*, 308(5723), 847-850.
43. Wild, M., Truessel, B., Ohmura, A., Long, C. N., & König-Langlo, G. (2013). The global radiation budget archive version 2.0. *Earth System Science Data*, 5(2), 213-220.

44. Wang, K., & Liang, S. (2009). Global atmospheric downward longwave radiation over land surface under all-sky conditions from 1973 to 2008. *Journal of Geophysical Research: Atmospheres*, 114(D19).
45. Wild, M., & Liepert, B. (2010). The Earth Radiation Balance as Driver of the Climate System: An Assessment from Satellite Observations. *Journal of Climate*, 23(3), 500-522.